Thin-Walled Structures 52 (2012) 102–116

Contents lists available at SciVerse ScienceDirect

Thin-Walled Structures

journal homepage: www.elsevier.com/locate/tws

A consistent total Lagrangian finite element for composite closed section thin walled beams

Martín C. Saravia *, Sebastián P. Machado, Víctor H. Cortínez

Centro de Investigación en Mecánica Teórica y Aplicada, CONICET—Universidad Tecnológica Nacional, Facultad Regional Bahía Blanca, 11 de Abril 461, 8000 Bahía Blanca, Argentina

ARTICLE INFO

Article history:
Received 13 July 2011
Received in revised form
8 November 2011
Accepted 16 November 2011
Available online 14 January 2012

Keywords:
Composite beams
Finite elements
Finite rotations
Thin-walled beams
Optimization

ABSTRACT

This work presents a consistent geometrically exact finite element formulation of the thin-walled anisotropic beam theory. The present formulation is thought to address problems of composite beams with nonlinear behavior. The constitutive formulation is based on the relations of composite laminates and thus the cross sectional stiffness matrix is obtained analytically. The variational formulation is written in terms of generalized strains, which are parametrized with the director field and its derivatives. The generalized strains and generalized beam forces are obtained by introducing a transformation that maps generalized components into physical components. A consistent tangent stiffness matrix is obtained by parametrizing the finite rotations with the total rotation vector; its derivation is greatly simplified by obtention of the derivatives of the director field via interpolation of nodal triads. Several numerical examples are presented to show the accuracy of the formulation and also its frame invariance and path independence.

1. Introduction

The study of the mechanics of modern high aspect ratio wings involves two main difficulties; on one hand, the modeling of the material behavior and, on the other hand, the treatment of finite deformations. In the last years, shell theories were often preferred over beam theories to address these problems. This was greatly helped by the increment in power of computers and the development of the finite element method.

Nowadays the scenario is changing, optimization techniques are widely being applied to the design of modern structures; and of course high aspect ratio wings are not an exception. This turned the attention back to beam theories, first because heuristic optimization techniques require massive computations and beam theories are less resources consuming. In addition, the requisite of optimization target functions containing analytical expressions for the cross section stiffness also represents an advantage of beam formulations. Thus, modern design of high aspect ratio wings could be facilitated by a beam finite element formulation capable of representing accurately the material and the kinematic behavior of the structure as well as feeding the optimization algorithms.

Commonly, the geometrically linear composite thin-walled beam theories produce accurate results when modeling wings that suffer small deformation. High aspect ratio composite wings normally suffer finite deformation; this demands a good knowledge of geometrical nonlinearities, which considerably complicates the formulation of the problem. Because of that, most of the reported composite thin-walled formulations only treat approximately such geometrical nonlinearities. Sometimes such approximations are not sufficient and higher order theories are needed. In view of this, the present work presents a geometrically exact beam finite element based on the composite thin-walled beam theory.

A geometrically exact beam theory must provide the exact relations between the configuration and the strains in a fully consistent manner with the virtual work principle regardless of the magnitude of the kinematic variables chosen to parametrize the configuration. Unfortunately, this task is not trivial and the consideration of 3D finite rotations introduces a great complexity to the kinematic description of a beam.

Several authors have studied geometrically exact beam finite element formulations. As a starting point, Reissner provided a 2D exact beam theory capable of describing arbitrary large displacements and rotations and a 3D theory for second order rotations [1].

Updated and Total Lagrangian formulations valid for large displacements and based on a degenerate continuum concept were presented by Bathe and Bolourchi [2].

Simo [3] and Simo and Vu-Quoc [4,5] developed the first 3D geometrically exact formulation for isotropic hyperelastic beams.

* Corresponding author.
E-mail address: msaravia@conicet.gov.ar (M.C. Saravia).

0263-8231/$ - see front matter © 2011 Elsevier Ltd. All rights reserved.
doi:10.1016/j.tws.2011.11.007

They used the Reissner relationships between the variation of the rotation tensor and the infinitesimal rotations to derive the strain-configuration relations, maintaining the geometric exactness of the theory. Simo [3] parametrized the finite rotations with the rotation tensor, aided by the quaternion algebra to enhance the computational efficiency of the algorithm. He proposed a multiplicative updating procedure for the rotational changes, obtaining a non-symmetrical tangent stiffness.

Another important contribution to the subject was done by Cardona and Geradin [6], who presented a different alternative of parametrization, they used the incremental Cartesian rotation vector to update the 3D rotations on the basis of the initial configuration. This approach updates the configuration on the basis of the last converged configuration. The additive treatment of the rotational degrees of freedom gives rise to a symmetrical tangent stiffness. An isotropic hyperelastic constitutive law was assumed.

Simo and Vu-Quoc [7] incorporated shear and torsion warping deformation effects in his geometrically exact model. An extension of the formulation of Simo to curved beams was presented by Ibrahimbegovic [8]. He extended the formulation to arbitrary curved space beams maintaining some key aspects of Simo formulation but using hierarchical interpolation. He also proposed an incremental rotation vector formulation [9] to solve the nonlinear dynamics of space beams.

The use of the Green–Lagrange strain measures in a geometrically exact finite element formulation for 3D beams seems to have been introduced by Gruttmann [10,11]. He obtained a formation parametrized in terms of directors at the integration point, the formulation was greatly simplified by the elimination of high order strains. In the same direction, Auricchio [12] reviewed the Simo theory making equivalence between Green–Lagrange strain measures and Reissner strain measures.

During the last years, great efforts were made to shed light to the problem of loss of objectivity introduced by the interpolation of rotations variables, a problem first noted by Crisfield and Jelenic [13]. Jelenic and Crisfield [14] implemented the ideas proposed in [13] to complete the development of a strain-invariant and path independent geometrically exact 3D beam element. Also Ibrahimbegovic and Taylor [15] re-examine the geometrically exact models to clarify the frame invariance issues concerning multiplicative and additive updates of rotations. Betsch and Steinmann [16], Armero and Romero [17] and Romero and Armero [18] further contributed to the subject presenting frame-invariant formulations for geometrically exact beams using the director field to parametrize the equations of motion. In these works, the directors were obtained through parametrization with spatial spins; thus, the obtained tangent stiffness matrices were non-consistent. Additional treatment of frame invariance can be found in Refs. [19,20]. Makinen [21] developed a Total Lagrangian formulation for isotropic materials. Besides obtaining a consistent stiffness matrix formulated in terms Reissner strains and total rotations, he demonstrated that some conclusions presented in [14] regarding the frame-invariance of Total Lagrangian formulations were incorrect. This misconception was caused by the wrong assumption that linear interpolation of total rotations is preserved under rigid body rotations.

All the aforementioned formulations deal with isotropic beams with solid cross section. As a consequence, its extension to composite thin-walled beams is not trivial. The advantage of thin-walled beam formulations is that the inclusion of material anisotropy is greatly facilitated. The inclusion of anisotropic materials to thin-walled and also solid beam finite element formulations was extensively studied by Hodges [22]. His work is based on the Variational Asymptotic Method (VAM) and deserves special attention. Besides several interesting developments, he and his coworkers developed a geometrically exact, fully intrinsic theory for the dynamics of curved and twisted composite beams, having neither displacements nor rotations appearing in the formulation. Using the VAM, a generalized Vlasov theory for composite beams based on the variational asymptotic beam sectional analysis was also presented by Yu et al. [23]. These developments were helped by the Variational Asymptotic Beam Sectional Analysis software (VABS) [24], a tool for obtaining thin-walled composite beams sectional properties. VABS is based on a 2D finite element analysis of the cross section to obtain the stiffness matrix of the underlying 1D theory.

An extensive review on analytical methods for solving geometrically nonlinear problems of composite thin-walled beams was done by Librescu [25]. He used different analytical approaches to treat composite beams undergoing moderate rotations, treating rotation variables in a vectorial fashion. Piovan and Cortínez [26] and Machado [27] presented a formulation for composite beams undergoing moderate rotations. Both formulations rely on an assumed displacement field and treat rotations as vectors, which confuses the actual meaning of these variables and also introduces uncertainty to the formulation.

In the context of thin-walled composite beams, Saravia et al. [28] presented a geometrically exact formulation for thin-walled composite beams using a parametrization in terms of director vectors. This formulation used spins as rotation variables, thus obtaining an unsymmetrical tangent stiffness. The resulting finite element implementation was path dependent and non-invariant.

This work presents a frame invariant and path independent finite element formulation of the thin-walled anisotropic beam theory. The obtention of the cross sectional stiffness matrices is based on the classical lamination theory and thus can handle any type of composite material. The cross section stiffness is thus obtained analytically and without the necessity of performing a 2D finite element cross sectional analysis. This opens the possibility of addressing optimization problems where it is desired to include the cross sectional shape in the target functions.

The parametrization of the finite rotation is done with the total rotation vector. In the present formulation we use interpolation to obtain the derivatives of the director field, thus avoiding the need of the derivatives of the rotation variables. This greatly simplifies the derivation of the linearization of the Green–Lagrange strains. Since the variational formulation is expressed in terms of director field there is no need of reparametrization, this is in contrast to the works in [11,16–18] where the Reissner strain measures must be reparametrized.

Regarding the objectivity and path independence of geometrically exact formulations, it has been shown that in the presence of finite three dimensional rotations the concept of objectivity of strain measures does not extend naturally from the theory to the finite element formulation [13]. Hence, despite being some formulations frame indifferent, they suffer from interpolation induced non-objectivity. We demonstrate that in the present formulation the discrete generalized strains satisfy the frame invariance property and that the implementation is path independent. Also, it is shown that although other director parametrized formulations resulted to be frame invariant and path independent [16–18], the obtained stiffness matrices were not consistent. We also show that it is not possible to obtain a consistent geometrical stiffness matrix completely avoiding the use of interpolation of the rotation. Finally, several examples show the present implementation has a very good correlation against 3D anisotropic shell theory.

2. Kinematics

The kinematic description of the beam is extracted from the relations between two states of a beam, an undeformed reference

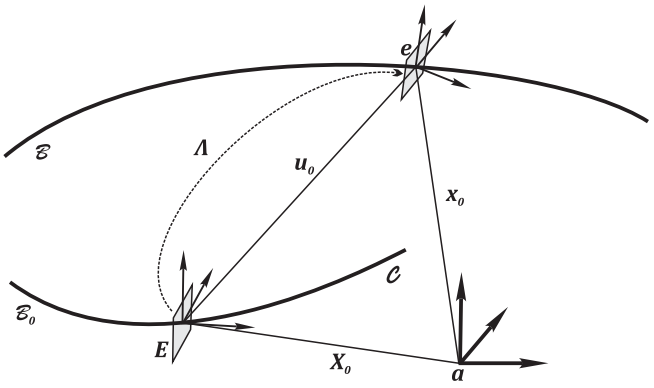

Fig. 1. 3D beam kinematics.

state (denoted as $\mathcal{B}_0$) and a deformed state (denoted as $\mathcal{B}$), as it is shown in Fig. 1. Being $\boldsymbol{a}_i$ a spatial frame of reference, we define two orthonormal frames: a reference frame $\boldsymbol{E}_i$ and a current frame $\boldsymbol{e}_i$.

The displacement of a point in the deformed beam measured with respect to the undeformed reference state can be expressed in the global coordinate system $\boldsymbol{a}_i$ in terms of a vector $\boldsymbol{u}=(u_1,u_2,u_3)$.

The current frame $\boldsymbol{e}_i$ is a function of a running length coordinate along the reference line of the beam, denoted as x, and is fixed to the beam cross-section. For convenience, we choose the reference curve $\mathcal{C}$ to be the locus of cross-sectional inertia centroids. The origin of $\boldsymbol{e}_i$ is located on the reference line of the beam and is called *pole*. The cross-section of the beam is arbitrary and initially normal to the reference line.

The relations between the orthonormal frames are given by the linear transformations:

$$\boldsymbol{E}_i=\boldsymbol{\Lambda}_0(x)\boldsymbol{a}_i,\quad \boldsymbol{e}_i=\boldsymbol{\Lambda}(x)\boldsymbol{E}_i, \tag{1}$$

where $\boldsymbol{\Lambda}_0(x)$ and $\boldsymbol{\Lambda}(x)$ are two-point tensor fields $\in$SO(3); the special orthogonal (Lie) group. Thus, it is satisfied that $\boldsymbol{\Lambda}_0^{\boldsymbol{T}}\boldsymbol{\Lambda}_0=\boldsymbol{I}$, $\boldsymbol{\Lambda}^{\boldsymbol{T}}\boldsymbol{\Lambda}=\boldsymbol{I}$. We will consider that the beam element is straight, so we set $\boldsymbol{\Lambda}_0=I$.

Recalling the relations (1), we can express the position vectors of a point in the beam in the undeformed and deformed configuration, respectively, as

$$\boldsymbol{X}(x,\xi_2,\xi_3)=\boldsymbol{X}_0(x)+\sum_{i=2}^{3}\xi_i\boldsymbol{E}_i,\quad \boldsymbol{x}(x,\xi_2,\xi_3,t)=\boldsymbol{x}_0(x,t)+\sum_{i=2}^{3}\xi_i\boldsymbol{e}_i. \tag{2}$$

Where in both equations the first term stands for the position of the pole and the second term stands for the position of a point in the cross section relative to the pole. Note that x is the running length coordinate and ξ_2 and ξ_3 are cross section coordinates. At this point we note that since the present formulation is thought to be used for modeling high aspect ratio composite beams, the warping displacement is not included. As it is widely known, for such type of beams the warping effect is negligible [29].

Also, it is possible to express the displacement field as

$$\boldsymbol{U}(x,\xi_2,\xi_3,t)=\boldsymbol{x}-\boldsymbol{X}=\boldsymbol{u}(x,t)+(\boldsymbol{\Lambda}-\mathbf{I})\sum_{2}^{3}\xi_i\boldsymbol{E}_i, \tag{3}$$

where $\boldsymbol{u}$ represents the displacement of the kinematic center of reduction, i.e. the pole. The nonlinear manifold of 3D rotation transformations $\boldsymbol{\Lambda}(\boldsymbol{\theta})$ (belonging to the special orthogonal Lie Group SO(3)) is described mathematically via the exponential map as

$$\boldsymbol{\Lambda}(\boldsymbol{\theta})=\cos\theta\boldsymbol{I}+\frac{\sin\theta}{\theta}\boldsymbol{\Theta}+\frac{1-\cos\theta}{\theta^2}\boldsymbol{\theta}\otimes\boldsymbol{\theta}, \tag{4}$$

where $\boldsymbol{\theta}=[\theta_1\ \theta_2\ \theta_3]^T$ is the rotation vector, θ its modulus and $\boldsymbol{\Theta}$ is its skew symmetric matrix (often called *spinor*). Euler's theorem states that when a rigid body rotates from one orientation to another, which may be the result of a series of rotations (with one rotation superposed onto the previous), the total rotation can be seen as single (compound) rotation about some spatial fixed axis $\boldsymbol{\theta}$ (see e.g. [30]). Therefore, the rotation vector can be understood as a compound rotation that globally or totally parametrizes the compound rotation tensor via Eq. (4).

The set of kinematic variables is formed by three displacements and three rotations as

$$\mathcal{V}:=\{\phi=[\boldsymbol{u},\boldsymbol{\theta}]^T:[0,\ell]\to R^3\},\quad [\boldsymbol{u},\boldsymbol{\theta}]^T=[u_1,u_2,u_3,\theta_1,\theta_2,\theta_3]^T. \tag{5}$$

Considering the effects of transverse shear strains gives, in general, $\boldsymbol{e}_1\cdot\boldsymbol{x}_{,1}>0$.

3. Beam mechanics

3.1. Strain field

In this section we present the strain field obtained when feeding the Green–Lagrange (GL) strain tensor with the kinematics. So, we need to express the GL strain tensor in terms of reference and current position derivatives. First, we obtain the derivatives of the position vectors of the undeformed and deformed configurations as

$$\begin{aligned}
&\boldsymbol{X}_{,1}=\boldsymbol{X}_0'+\xi_2\boldsymbol{E}_2'+\xi_3\boldsymbol{E}_3', && \boldsymbol{x}_{,1}=\boldsymbol{x}_0'+\xi_2\boldsymbol{e}_2'+\xi_3\boldsymbol{e}_3',\\
&\boldsymbol{X}_{,2}=\boldsymbol{E}_2, && \boldsymbol{x}_{,2}=\boldsymbol{e}_2,\\
&\boldsymbol{X}_{,3}=\boldsymbol{E}_3, && \boldsymbol{x}_{,3}=\boldsymbol{e}_3.
\end{aligned} \tag{6}$$

Note that we have implicitly made the classical assumption of beam theories of plane cross-sections remaining plane. Proceeding with the derivation, we operate in a conventional way by injecting the tangent vectors $\boldsymbol{X}_{,i}$ and $\boldsymbol{x}_{,i}$ into the GL strain expression $\boldsymbol{E}_{GL}=(1/2)(\boldsymbol{x}_{,i}\cdot\boldsymbol{x}_{,j}-\boldsymbol{X}_{,i}\cdot\boldsymbol{X}_{,j})$ [31].

According to the kinematic hypotheses, the non-vanishing components of the GL strain vector are only three. In vector notation, it gives: $\boldsymbol{E}_{GL}=[E_{11}\ 2E_{12}\ 2E_{13}]^T$, where

$$\begin{aligned}
E_{11}&=\frac{1}{2}(\boldsymbol{x}_0'^2-\boldsymbol{X}_0'^2)+\xi_2(\boldsymbol{x}_0'\cdot\boldsymbol{e}_3'-\boldsymbol{X}_0'\cdot\boldsymbol{E}_3')+\xi_3(\boldsymbol{x}_0'\cdot\boldsymbol{e}_2'-\boldsymbol{X}_0'\cdot\boldsymbol{E}_2')\\
&\quad+\frac{1}{2}\xi_2^2(\boldsymbol{e}_2'^2-\boldsymbol{E}_2'^2)+\frac{1}{2}\xi_3^2(\boldsymbol{e}_3'^2-\boldsymbol{E}_3'^2)+\xi_2\xi_3(\boldsymbol{e}_2'\cdot\boldsymbol{e}_3'-\boldsymbol{E}_2'\cdot\boldsymbol{E}_3'),\\
E_{12}&=\frac{1}{2}[\boldsymbol{x}_0'\cdot\boldsymbol{e}_2-\boldsymbol{X}_0'\cdot\boldsymbol{E}_2-\xi_3(\boldsymbol{e}_3'\cdot\boldsymbol{e}_2-\boldsymbol{E}_3'\cdot\boldsymbol{E}_2)],\\
E_{13}&=\frac{1}{2}[\boldsymbol{x}_0'\cdot\boldsymbol{e}_3-\boldsymbol{X}_0'\cdot\boldsymbol{E}_3+\xi_2(\boldsymbol{e}_2'\cdot\boldsymbol{e}_3-\boldsymbol{E}_2'\cdot\boldsymbol{E}_3)].
\end{aligned} \tag{7}$$

To simplify the derivation of the thin-walled beam strains we introduce now the *generalized strain vector* $\boldsymbol{\varepsilon}$, a vector that properly transformed gives the GL strain vector. This transformation actually "extracts" from the GL strain vector the variables related to the location of a point in the cross section (i.e. ξ_i). Therefore, the mentioned transformation is written as

$$\boldsymbol{E}_{GL}=D\boldsymbol{\varepsilon}, \tag{8}$$

where the transformation matrix is

$$\boldsymbol{D}=\begin{bmatrix}
1 & \xi_3 & \xi_2 & 0 & 0 & 0 & \frac{1}{2}\xi_2^2 & \frac{1}{2}\xi_3^2 & \xi_2\xi_3\\
0 & 0 & 0 & 1 & 0 & -\xi_3 & 0 & 0 & 0\\
0 & 0 & 0 & 0 & 1 & \xi_2 & 0 & 0 & 0
\end{bmatrix}. \tag{9}$$

And the generalized strain vector is

$$\boldsymbol{\varepsilon}=\begin{bmatrix}\epsilon\\ \kappa_2\\ \kappa_3\\ \gamma_2\\ \gamma_3\\ \kappa_1\\ \chi_2\\ \chi_3\\ \chi_{23}\end{bmatrix}=\begin{bmatrix}\frac{1}{2}(\boldsymbol{x}_0'\cdot\boldsymbol{x}_0'-\boldsymbol{X}_0'\cdot\boldsymbol{X}_0')\\ \boldsymbol{x}_0'\cdot\boldsymbol{e}_3'-\boldsymbol{X}_0'\cdot\boldsymbol{E}_3'\\ \boldsymbol{x}_0'\cdot\boldsymbol{e}_2'-\boldsymbol{X}_0'\cdot\boldsymbol{E}_2'\\ \boldsymbol{x}_0'\cdot\boldsymbol{e}_2-\boldsymbol{X}_0'\cdot\boldsymbol{E}_2\\ \boldsymbol{x}_0'\cdot\boldsymbol{e}_3-\boldsymbol{X}_0'\cdot\boldsymbol{E}_3\\ \boldsymbol{e}_2'\cdot\boldsymbol{e}_3-\boldsymbol{E}_2'\cdot\boldsymbol{E}_3\\ \boldsymbol{e}_2'\cdot\boldsymbol{e}_2'-\boldsymbol{E}_2'\cdot\boldsymbol{E}_2'\\ \boldsymbol{e}_3'\cdot\boldsymbol{e}_3'-\boldsymbol{E}_3'\cdot\boldsymbol{E}_3'\\ \boldsymbol{e}_2'\cdot\boldsymbol{e}_3'-\boldsymbol{E}_2'\cdot\boldsymbol{E}_3'\end{bmatrix}. \tag{10}$$

As it can be observed, the generalized strain vector $\boldsymbol{\varepsilon}$ contains nine generalized beam strains which belong to a material description and are expressed in a rectangular coordinate system. The physical meaning of the generalized strain is: ϵ measures the axial strain of the reference line of the beam, κ_2 and κ_3 are the flexural curvatures, γ_2 and γ_3 are the shear strains and κ_1 is the rate of twist or torsional curvature. The meaning of the higher order strains is a little more involved: χ_2, χ_3, measure both torsional and flexural strains and also torsional–flexural coupling and flexural–flexural coupling strains. The last term χ_{23} is a flexural–flexural and torsional–flexural coupling strain.

The derivation of strain and stress measures is helped by the introduction of an orthogonal curvilinear coordinate system (x,n,s), see Fig. 2. The cross-section shape will be defined in this coordinate system by functions $\xi_i(n,s)$. The coordinate s is measured along the tangent to the middle line of the cross section, in clockwise direction and with origin conveniently chosen. Besides, the thickness coordinate $n(-e/2\le e/2)$ is perpendicular to s and with origin in the middle line contour.

In order to represent the GL strains in this curvilinear coordinate system we make use of the transformation tensor

$$\boldsymbol{P}=\begin{bmatrix}1 & 0 & 0\\ 0 & \frac{d\overline{\xi}_2}{ds} & \frac{d\overline{\xi}_3}{ds}\\ 0 & -\frac{d\overline{\xi}_3}{ds} & \frac{d\overline{\xi}_2}{ds}\end{bmatrix}, \tag{11}$$

where the functions $\overline{\xi}_i$ describe the mid-contour of the cross section.

Hence, the GL strain vector in the curvilinear coordinate system is obtained by transforming the rectangular GL strains as

$$\hat{\boldsymbol{E}}_{GL}=[E_{xx}\ \ 2E_{xs}\ \ 2E_{xn}]^T=\boldsymbol{P}\boldsymbol{E}_{GL}, \tag{12}$$

The curvilinear GL strain vector can then be expressed as

$$\hat{\boldsymbol{E}}_{GL}=\boldsymbol{P}\boldsymbol{D}\boldsymbol{\varepsilon} \tag{13}$$

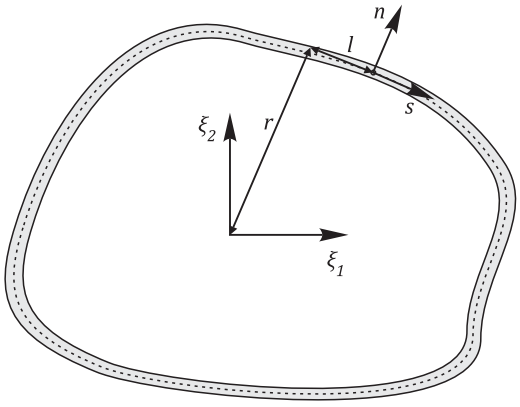

Fig. 2. Curvilinear transformation schematic.

Recalling Eqs. (9) and (10), it is found that the GL strain vector in curvilinear coordinates has a remarkably simple closed expression

$$\hat{\boldsymbol{E}}_{GL}=\begin{bmatrix}\epsilon+\xi_2\kappa_3+\xi_3\kappa_2+\frac{1}{2}\xi_2^2\chi_2+\frac{1}{2}\xi_3^2\chi_3+\xi_2\xi_3\chi_{23}\\ \overline{\xi}_2'\gamma_2+\overline{\xi}_3'\gamma_3+(\xi_2\overline{\xi}_3'-\xi_3\overline{\xi}_2')\kappa_1\\ -\overline{\xi}_3'\gamma_2+\overline{\xi}_2'\gamma_3+(\xi_2\overline{\xi}_2'+\xi_3\overline{\xi}_3')\kappa_1\end{bmatrix}, \tag{14}$$

where the prime symbol has been used to denote derivation with respect to the s coordinate.

Now we can refer to Fig. 2 (see also [27]) to easily verify that the location of a point anywhere in the cross-section can be expressed as

$$\xi_2(n,s)=\overline{\xi}_2(s)-n\frac{d\overline{\xi}_3}{ds},\ \ \xi_3(n,s)=\overline{\xi}_3(s)+n\frac{d\overline{\xi}_2}{ds}, \tag{15}$$

where $\overline{\xi}_i$ locates the points lying in the middle-line contour.

As it will be further clarified in the next section, we will use five independent curvilinear strain measures (collected in the vector $\boldsymbol{\epsilon}_s$) to describe the strain state of the thin-walled beam laminate (see [32]) as

$$\boldsymbol{\epsilon}_s=\begin{bmatrix}\varepsilon_{xx} & \gamma_{xs} & \gamma_{xn} & \varkappa_{xx} & \varkappa_{xs}\end{bmatrix}^T. \tag{16}$$

Pursuing the mentioned objective of describing the strain state of the beam in terms of the generalized strain vector, we first move to an intermediate step and introduce Eq. (15) into Eq. (14) to express the GL strains as a function of the mid-surface coordinates $\overline{\xi}_i$ and its derivatives. After doing that we found that a matrix $\boldsymbol{\mathcal{T}}$ establishes the relationship between the GL curvilinear strains and the generalized strains as

$$\boldsymbol{\epsilon}_s=\boldsymbol{\mathcal{T}}\boldsymbol{\varepsilon}. \tag{17}$$

Substituting Eq. (15) into Eq. (14) and neglecting higher order terms in the thickness (terms in n^2) we obtain

$$\boldsymbol{\mathcal{T}}(s)=\begin{bmatrix}1 & \overline{\xi}_3 & \overline{\xi}_2 & 0 & 0 & 0 & \frac{1}{2}\overline{\xi}_2^2 & \frac{1}{2}\overline{\xi}_3^2 & \overline{\xi}_2\overline{\xi}_3\\ 0 & 0 & 0 & \overline{\xi}_2' & \overline{\xi}_3' & \overline{\xi}_2\overline{\xi}_3'-\overline{\xi}_3\overline{\xi}_2' & 0 & 0 & 0\\ 0 & 0 & 0 & -\overline{\xi}_3' & \overline{\xi}_3^2 & \overline{\xi}_2\overline{\xi}_2'+\overline{\xi}_3\overline{\xi}_3' & 0 & 0 & 0\\ 0 & \overline{\xi}_2' & -\overline{\xi}_3' & 0 & 0 & 0 & -\overline{\xi}_2\overline{\xi}_3' & \overline{\xi}_3\overline{\xi}_2' & (\overline{\xi}_2\overline{\xi}_2'-\overline{\xi}_3\overline{\xi}_3')\\ 0 & 0 & 0 & 0 & 0 & -(\overline{\xi}_2'^2+\overline{\xi}_3'^2) & 0 & 0 & 0\end{bmatrix}. \tag{18}$$

It is interesting to note that the matrix $\boldsymbol{\mathcal{T}}$ plays the role of a double transformation matrix that directly maps the generalized strains $\boldsymbol{\varepsilon}$ into the curvilinear GL strain $\boldsymbol{\epsilon}_s$ without the necessity of an intermediate transformation.

Now, it is straightforward to obtain the curvilinear strains as a function of mid-contour quantities and the generalized strains as

$$\epsilon_s=\begin{bmatrix}\epsilon+\kappa_3\overline{\xi}_2++\kappa_2\overline{\xi}_3+0.5\chi_2\overline{\xi}_2^2+\chi_{23}\overline{\xi}_2\overline{\xi}_3+0.5\chi_3\overline{\xi}_3^2\\ \gamma_2\overline{\xi}_2'+\gamma_3\overline{\xi}_3'+\kappa_1(\overline{\xi}_3'\overline{\xi}_2-\overline{\xi}_2'\overline{\xi}_3)\\ \gamma_3\overline{\xi}_2'-\gamma_2\overline{\xi}_3'+\kappa_1(\overline{\xi}_2'\overline{\xi}_2+\overline{\xi}_3'\overline{\xi}_3)\\ \kappa_2\overline{\xi}_2'-\kappa_3\overline{\xi}_3'-\chi_2\overline{\xi}_3'\overline{\xi}_2+\chi_3\overline{\xi}_2'\overline{\xi}_3+\chi_{23}(\overline{\xi}_2'\overline{\xi}_2-\overline{\xi}_3'\overline{\xi}_3)\\ \kappa_1(-\overline{\xi}_2'^2-\overline{\xi}_3'^2)\end{bmatrix} \tag{19}$$

3.2. Constitutive relations

The most interesting capability of the present formulation is to handle composite materials in a geometrically exact framework without modifying the classical thin-walled beam approach. In this section we present the equations that describe the mechanics of the composite material. The reduction to the isotropic case is straightforward.

For an orthotropic lamina, the relationship between the second Piola–Kirchhoff stress tensor and its energetic conjugate;

the GL strain tensor, can be expressed in curvilinear coordinates as a matrix of stiffness coefficients Q_{ij} [32–33]

$$\begin{bmatrix}\sigma_{xx}\\ \sigma_{ss}\\ \sigma_{nn}\\ \sigma_{sn}\\ \sigma_{xn}\\ \sigma_{xs}\end{bmatrix}=\begin{bmatrix}Q_{11} & Q_{12} & Q_{13} & 0 & 0 & Q_{16}\\ Q_{12} & Q_{22} & Q_{23} & 0 & 0 & Q_{26}\\ Q_{13} & Q_{23} & Q_{33} & 0 & 0 & Q_{36}\\ 0 & 0 & 0 & Q_{44} & Q_{45} & 0\\ 0 & 0 & 0 & Q_{45} & Q_{55} & 0\\ Q_{16} & Q_{26} & Q_{36} & 0 & 0 & Q_{66}\end{bmatrix}\begin{bmatrix}\epsilon_{xx}\\ \epsilon_{ss}\\ \epsilon_{nn}\\ \gamma_{sn}\\ \gamma_{xn}\\ \gamma_{xs}\end{bmatrix}. \tag{20}$$

In matrix form

$$\boldsymbol{\sigma}=\boldsymbol{Q}\boldsymbol{\epsilon}_s. \tag{21}$$

In the above equation Q_{ij} are components of the *transformed constitutive (or stiffness) matrix* defined in terms of the elastic properties (elasticity moduli and Poisson coefficients) and fiber orientation of the ply [32].

The shell stress resultants in a lamina result from the integration of 3D stresses in the thickness, and are thus defined as

$$N_{ij}=\int_{-e/2}^{e/2}\sigma_{ij}dn,\quad M_{ij}=\int_{-e/2}^{e/2}\sigma_{ij}n\,dn. \tag{22}$$

Employing Eqs. (20) and (22) and neglecting the normal stress in the thickness (i.e. $\sigma_{nn}=0$) it is possible to obtain a constitutive relation between the shell forces and strains as

$$\begin{bmatrix}N_{xx}\\ N_{ss}\\ N_{xs}\\ N_{sn}\\ N_{xn}\\ M_{xx}\\ M_{ss}\\ M_{xs}\end{bmatrix}=\begin{bmatrix}A_{11} & A_{12} & A_{13} & 0 & 0 & B_{11} & B_{12} & B_{16}\\ A_{12} & A_{22} & A_{23} & 0 & 0 & B_{12} & B_{22} & B_{26}\\ A_{13} & A_{23} & A_{33} & 0 & 0 & B_{16} & B_{26} & B_{66}\\ 0 & 0 & 0 & A_{44}^H & A_{45}^H & 0 & 0 & 0\\ 0 & 0 & 0 & A_{45}^H & A_{55}^H & 0 & 0 & 0\\ B_{11} & B_{12} & B_{16} & 0 & 0 & D_{11} & D_{12} & D_{16}\\ B_{12} & B_{22} & B_{26} & 0 & 0 & D_{12} & D_{22} & D_{26}\\ B_{16} & B_{26} & B_{66} & 0 & 0 & D_{16} & D_{26} & D_{66}\end{bmatrix}\begin{bmatrix}\epsilon_{xx}\\ \epsilon_{ss}\\ \gamma_{xs}\\ \gamma_{sn}\\ \gamma_{xn}\\ \kappa_{xx}\\ \kappa_{ss}\\ \kappa_{xs}\end{bmatrix}, \tag{23}$$

where N_{xx}, N_{ss}, and N_{xs} are axial, hoop and shear-membrane shell forces, respectively, and N_{xn} and N_{sn} are transverse shear shell forces. Also M_{xx}, M_{ss} and M_{xs} are axial bending, hoop bending and twisting shell moments, respectively. The same nomenclature is extended to the shell strain resultants, thus ε_{xx} and ε_{ss} are axial and hoop normal strains, respectively, γ_{xs}, γ_{sn} and γ_{xn} are shear shell strains and $\varkappa_{xx}$, $\varkappa_{ss}$ and $\varkappa_{xs}$ are axial, hoop and twisting curvatures, respectively. The coefficients A_{ij}, A_{ij}^H, B_{ij} and D_{ij} in the constitutive matrix are shell stiffness-coefficients that result from the integration of Q_{ij} in the thickness [32].

Although the last relationships were derived for a single lamina, we can obtain the constitutive relations for a laminate by spanning the integrals in the thickness of the lamina over the different layers of the laminate (each layer being a single lamina). Therefore, using the hypotheses of plane stress in the laminate and rigid cross section the relations 0 simplify to

$$\begin{bmatrix}N_{xx}\\ N_{xs}\\ N_{xn}\\ M_{xx}\\ M_{xs}\end{bmatrix}=\begin{bmatrix}\overline{A}_{11} & \overline{A}_{16} & 0 & \overline{B}_{11} & \overline{B}_{16}\\ \overline{A}_{16} & \overline{A}_{66} & 0 & \overline{B}_{16} & \overline{B}_{66}\\ 0 & 0 & \overline{A}_{55}^H & 0 & 0\\ \overline{B}_{11} & \overline{B}_{16} & 0 & \overline{D}_{11} & \overline{D}_{16}\\ \overline{B}_{16} & \overline{B}_{66} & 0 & \overline{D}_{16} & \overline{D}_{66}\end{bmatrix}\begin{bmatrix}\varepsilon_{xx}\\ \gamma_{xs}\\ \gamma_{xn}\\ \varkappa_{xx}\\ \varkappa_{xs}\end{bmatrix}, \tag{24}$$

where $\overline{A}_{ij}$ are components of the laminate reduced in-plane stiffness matrix, $\overline{B}_{ij}$ are components of the reduced bending-extension coupling matrix, $\overline{D}_{ij}$ are components of the reduced bending stiffness matrix and $\overline{A}_{55}^H$ is the component of the reduced transverse shear stiffness matrix.

It must be noted that according to the plane stress hypothesis $\varepsilon_{ss}=\gamma_{ns}=0$, but in order to avoid overstiffening effects we set $N_{ss}=\gamma_{ns}=0$ [32]. This generates a mild inconsistency typical of thin-walled beam formulations

We can express the above relation in matrix form as

$$\boldsymbol{N}_s=\boldsymbol{C}\boldsymbol{\epsilon}_s, \tag{25}$$

where $\boldsymbol{C}$ is the composite shell constitutive matrix and $\boldsymbol{\epsilon}_s$ is the curvilinear shell strain vector defined in Eq. (17).

3.3. Beam forces

The objective of this subsection is to reduce the 2D formulation to a 1D formulation. In order to do that, it is first necessary to express the shell forces as a function of the generalized strains. Replacing Eq. (17) into Eq. (25) we obtain

$$\boldsymbol{N}_s=\boldsymbol{C}\boldsymbol{\mathcal{T}}\boldsymbol{\varepsilon}. \tag{26}$$

Since we are pursuing to formulate the theory in terms of generalized quantities, we need to find a one dimensional stress (or force) entity such as to be work conjugate with the generalized strains. To that purpose, we first transform the shell forces in Eq. (26) back to the "generalized space" using the double transformation matrix $\boldsymbol{\mathcal{T}}$. Hence, we obtain the transformed back shell strain as

$$\boldsymbol{N}_s^G=\boldsymbol{\mathcal{T}}^T\boldsymbol{N}_s=\boldsymbol{\mathcal{T}}^T\boldsymbol{C}\boldsymbol{\mathcal{T}}\boldsymbol{\varepsilon}. \tag{27}$$

We see that $\boldsymbol{N}_s^G$ is a vector of generalized shell stresses defined in the global coordinate system. It is a function of the cross section mid-contour and thus integration over the contour gives the vector of generalized beam forces (work conjugate with the generalized strains) as

$$\boldsymbol{S}(x)=\int_S\boldsymbol{N}_s^G ds=\left(\int_S\boldsymbol{\mathcal{T}}^T\boldsymbol{C}\boldsymbol{\mathcal{T}}\,ds\right)\boldsymbol{\varepsilon}(x), \tag{28}$$

$$\boldsymbol{S}(x)=\mathbb{D}\boldsymbol{\varepsilon}(x). \tag{29}$$

Note that since the generalized strain vector $\boldsymbol{\varepsilon}$ is not a function of the curvilinear coordinate s, (see Eq. (10)) it was taken out of the integral over the contour. So, the new matrix $\mathbb{D}$ was defined such that

$$\mathbb{D}=\int_S\boldsymbol{\mathcal{T}}^T\boldsymbol{C}\boldsymbol{\mathcal{T}}\,ds. \tag{30}$$

It is good to note that $\mathbb{D}$ contains functions $\overline{\xi}_i$ that define the cross section mid-contour and also all the anisotropic material constants. Besides, it contains not only all geometrical couplings but also all material couplings. Commonly, the functions $\overline{\xi}_i$ are defined as piecewise functions, and so the integral to evaluate $\mathbb{D}$ needs to be performed in a piecewise manner (see e.g. [25]).

The evaluation of beam constitutive matrix $\mathbb{D}$ does not involve a 2D finite element analysis of the cross section (as, for example, in the VABS approach [24]). Although the constitutive constants are not as accurate as that the ones obtained with the mentioned method, the present approach is simpler, faster and it also opens the possibility of addressing optimization problems of large deformation of thin-walled composite beams. A detailed study of the performance of both methods can be found in [29].

4. Variational formulation

The weak form of equilibrium of a three dimensional body $\mathcal{B}$ is given by [34,35]

$$G(\boldsymbol{\phi},\delta\boldsymbol{\phi})=\int_{\mathcal{B}_0}\boldsymbol{\sigma}\cdot\delta\boldsymbol{\epsilon}\,dV-\int_{\mathcal{B}_0}\boldsymbol{\rho}_0\boldsymbol{b}\cdot\delta\boldsymbol{\phi}\,dV-\int_\ell(\boldsymbol{p}\cdot\delta\boldsymbol{u}+\boldsymbol{m}\cdot\delta\boldsymbol{\theta})dx, \tag{31}$$

where $\boldsymbol{b}$, $\boldsymbol{p}$ and $\boldsymbol{m}$ are body forces, prescribed external forces and prescribed external moments respectively. $\boldsymbol{\epsilon}$ is the 3D GL strain

tensor, work conjugate to the second Piola–Kirchhoff stress tensor $\boldsymbol{\sigma}$. We note that $\boldsymbol{\sigma}$ could be defined in either a rectangular or a curvilinear coordinate system (such a distinction is, at least at this point, unnecessary).

To maintain the variational formulation parametrized in terms of the director field, its admissible variation must be found. Then the generalized virtual strains can be obtained; so the virtual work of the internal and external forces can be derived. Therefore, we aim to express the virtual work principle as a function of the generalized virtual strain vector and its work conjugate beam forces vector.

4.1. Finite rotations and director variations

There are various ways to parametrize finite rotations: Euler angles, a four parameter quaternion intrinsic representation [3,8], a three parameter rotational vector [6], etc. These parametrizations can be total or incremental, as well as their combinations, and they lead to multiplicative or additive updating procedures.

It is known that the parametrization of finite rotations with spins leads to a non-symmetric tangent matrix [4], although symmetry is recovered at equilibrium. This kind of parametrization has the advantage of giving very simple expressions for the tangent matrix but, as a consequence of the interpolation of spins, it has the drawback of being path dependent and non frame invariant [14]. On the other hand, using the rotational vector to parametrize finite rotations leads to a symmetric tangent matrix but its derivation can be more complicated due to the complexity of the linearization of the virtual strains.

In this work we choose to describe the finite rotation with the rotation vector. It will be shown that the properties of frame indifference and path independency are satisfied and some common difficulties arising from the linearization are easily overcome.

To obtain the generalized strains variations, the admissible variation of the director field is required. Remembering that we set $\boldsymbol{\Lambda}_0=\boldsymbol{I}$ and recalling Eq. (1), we can write

$$\delta\boldsymbol{e}_i=\delta(\boldsymbol{\Lambda}\boldsymbol{E}_i)=\delta\boldsymbol{\Lambda}\boldsymbol{E}_i. \tag{32}$$

The admissible variation of the rotation tensor (Lie variation) can be obtained introducing an infinitesimal virtual rotation superposed onto the existing finite rotation, see e.g. [36, 37]. This virtual rotation lies in the tangent space at $\boldsymbol{\Lambda}$ (spatial virtual rotation), or in the tangent space at $\boldsymbol{I}$ (material virtual rotation), and is represented by a skew symmetric matrix $\delta\boldsymbol{W}$, or $\delta\boldsymbol{\Psi}$, respectively (see Fig. 3). These variables are called "*spins*" [38].

To find the variation of the rotation tensor we first construct the perturbed rotation tensor by exponentiating the spatial spin as

$$\boldsymbol{\Lambda}_\epsilon=\exp(\epsilon\delta\boldsymbol{W})\boldsymbol{\Lambda}. \tag{33}$$

At this point we note that $\boldsymbol{\Lambda}$ is a two point tensor, it takes vectors from the tangent space in the initial configuration to the tangent space in the current configuration. Thus, we can use it to relate spatial and material spins as

$$\delta\boldsymbol{\Psi}=\boldsymbol{\Lambda}^T\delta W\boldsymbol{\Lambda},\quad \delta\boldsymbol{W}=\boldsymbol{\Lambda}\delta\boldsymbol{\Psi}\boldsymbol{\Lambda}^T. \tag{34}$$

From which we can write the material version of the kinematically admissible perturbed finite rotation tensor as

$$\boldsymbol{\Lambda}_\epsilon=\boldsymbol{\Lambda}\exp(\epsilon\delta\boldsymbol{\Psi}). \tag{35}$$

Enforcing the additive property to hold, it can be devised yet another way of constructing the perturbed finite rotation tensor. Making use of the rotation vector, it is proposed

$$\boldsymbol{\Lambda}_\epsilon=\exp(\boldsymbol{\Theta}+\epsilon\delta\boldsymbol{\Theta}). \tag{36}$$

Recalling Eq. (33) and remembering that $\boldsymbol{\Lambda}=\exp(\boldsymbol{\Theta})$ we find that

$$\exp(\boldsymbol{\Theta}+\epsilon\delta\boldsymbol{\Theta})=\exp(\epsilon\delta\boldsymbol{W})\exp(\boldsymbol{\Theta}), \tag{37}$$

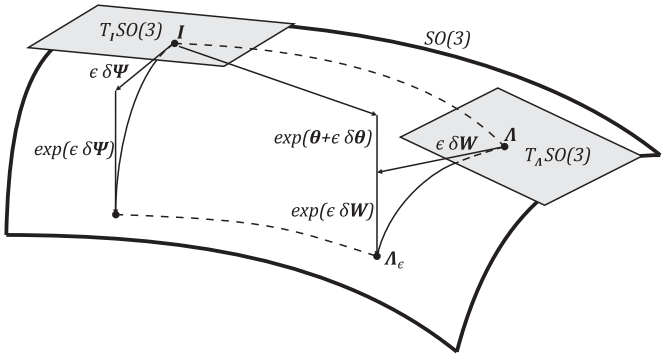

Fig. 3. Geometric interpretation of the exponential map.

where we are trying to find an incremental rotation tensor, i.e. the virtual rotation tensor $\delta\boldsymbol{\Theta}$, such that it belongs to the same tangent space as the rotation tensor $\boldsymbol{\Theta}$, i.e. $T_I SO(3)$. The vector $\boldsymbol{\theta}$ whose skew matrix is $\boldsymbol{\Theta}$ is the *total rotation vector*.

Taking derivatives with respect to the parameter ϵ we obtain (see e.g. [21,39])

$$\delta\boldsymbol{w}=\boldsymbol{T}\delta\boldsymbol{\theta}, \tag{38}$$

where $\boldsymbol{T}$ is the spatial tangential transformation

$$\boldsymbol{T}(\boldsymbol{\theta})=\frac{\sin\theta}{\theta}\boldsymbol{I}+\frac{1-\cos\theta}{\theta^2}\boldsymbol{\Theta}+\frac{\theta-\sin\theta}{\theta^3}\boldsymbol{\theta}\otimes\boldsymbol{\theta}. \tag{39}$$

These different choices for the construction of a kinematically admissible representation of the perturbed rotation tensor, together with the type of algorithm chosen to perform the configuration update, lead to different finite element formulations: Total Lagrangian, Updated Lagrangian and Eulerian formulations [6]. Since we chose the total rotation vector to parametrize the finite rotation, the present formulation is Total Lagrangian.

The weak form of the equations of motion was parametrized in terms of the current frame and its derivatives, to ease the derivation of the virtual work we use rotation variables that belong to the tangent space at $\boldsymbol{\Lambda}$. Considering the latter, we will use the spatial virtual rotation tensor (i.e. $\delta\boldsymbol{W}$) to obtain the kinematically admissible variation of the rotation tensor. Recalling Eq. (33) we can express the variation of the rotation tensor in terms of the spatial spin as

$$\delta\boldsymbol{\Lambda}=\frac{d}{d\epsilon}[\exp(\epsilon\delta\boldsymbol{W})\boldsymbol{\Lambda}]\big|_{\epsilon=0}=\delta W\boldsymbol{\Lambda}. \tag{40}$$

Again, $\delta\boldsymbol{W}$ is a skew symmetric matrix such that $\delta\boldsymbol{W}\boldsymbol{a}=\delta\boldsymbol{w}\times\boldsymbol{a}$. Therefore, we can rewrite Eq. (32) as

$$\delta\boldsymbol{e}_i=\delta\boldsymbol{w}\times\boldsymbol{e}_i. \tag{41}$$

Now, recalling Eq. (38), we can write the last equation as a function of the total rotation vector like

$$\delta\boldsymbol{e}_i=(\boldsymbol{T}\delta\boldsymbol{\theta})\times\boldsymbol{e}_i. \tag{42}$$

The set of kinematically admissible variations can now be defined as

$$\delta\mathcal{V}:=\{\delta\boldsymbol{\phi}=[\delta\boldsymbol{u},\delta\boldsymbol{\theta}]^T:[0,\ell]\to R^3\,|\,\delta\boldsymbol{\phi}=0\ \text{on}\ \mathcal{S}\}, \tag{43}$$

where $\mathcal{S}$ describes the boundaries with prescribed displacements and rotations.

To obtain the virtual generalized strains we will also need to find the variation of the derivative of the director field. Noting that $\boldsymbol{e}'=\boldsymbol{T}\boldsymbol{\theta}'$ we can find the variation of the director's

derivative as

$$\delta \boldsymbol{e}_i' = (\delta \boldsymbol{T}\boldsymbol{\theta}' + \boldsymbol{T}\delta\boldsymbol{\theta}') \times \boldsymbol{e}_i + (T\boldsymbol{\theta}') \times [(\boldsymbol{T}\delta\boldsymbol{\theta}) \times \boldsymbol{e}_i]. \tag{44}$$

4.2. Virtual generalized strains

The variations of the directors and its derivatives are now used to obtain the virtual generalized strains. Considering $\delta \boldsymbol{E}_i = 0$ and $\delta \boldsymbol{X}_0' = 0$ and performing the variation to Eq. (10) we obtain

$$\delta\boldsymbol{\varepsilon} = \begin{bmatrix} \boldsymbol{x}_0' \cdot \delta\boldsymbol{u}' \\ \boldsymbol{e}_3' \cdot \delta\boldsymbol{u}' + \boldsymbol{x}_0' \cdot \delta\boldsymbol{e}_3' \\ \boldsymbol{e}_2' \cdot \delta\boldsymbol{u}' + \boldsymbol{x}_0' \cdot \delta\boldsymbol{e}_2' \\ \boldsymbol{e}_2 \cdot \delta\boldsymbol{u}' + \boldsymbol{x}_0' \cdot \delta\boldsymbol{e}_2 \\ \boldsymbol{e}_3 \cdot \delta\boldsymbol{u}' + \boldsymbol{x}_0' \cdot \delta\boldsymbol{e}_3 \\ \delta\boldsymbol{e}_2' \cdot \boldsymbol{e}_3 + \boldsymbol{e}_2' \cdot \delta\boldsymbol{e}_3 \\ 2(\delta\boldsymbol{e}_2' \cdot \boldsymbol{e}_2') \\ 2(\delta\boldsymbol{e}_3' \cdot \boldsymbol{e}_3') \\ \delta\boldsymbol{e}_2' \cdot \boldsymbol{e}_3' + \boldsymbol{e}_2' \cdot \delta\boldsymbol{e}_3' \end{bmatrix}. \tag{45}$$

In order to maintain the compactness of the formulation, it will be useful to write the last expression as a function of a new set of kinematic variables $\delta\boldsymbol{\varphi}$ as

$$\delta\boldsymbol{\varepsilon} = \mathbb{H}\delta\boldsymbol{\varphi}. \tag{46}$$

where

$$\mathbb{H} = \begin{bmatrix} \boldsymbol{x}_0'^T & \boldsymbol{0} & \boldsymbol{0} & \boldsymbol{0} & \boldsymbol{0} & \boldsymbol{0} \\ \boldsymbol{e}_3'^T & \boldsymbol{0} & \boldsymbol{0} & \boldsymbol{0} & \boldsymbol{0} & \boldsymbol{x}_0'^T \\ \boldsymbol{e}_2'^T & \boldsymbol{0} & \boldsymbol{0} & \boldsymbol{0} & \boldsymbol{x}_0'^T & \boldsymbol{0} \\ \boldsymbol{e}_2^T & \boldsymbol{0} & \boldsymbol{x}_0'^T & \boldsymbol{0} & \boldsymbol{0} & \boldsymbol{0} \\ \boldsymbol{e}_3^T & \boldsymbol{0} & \boldsymbol{0} & \boldsymbol{x}_0'^T & \boldsymbol{0} & \boldsymbol{0} \\ \boldsymbol{0} & \boldsymbol{0} & \boldsymbol{0} & \boldsymbol{e}_2'^T & \boldsymbol{e}_3^T & \boldsymbol{0} \\ \boldsymbol{0} & \boldsymbol{0} & \boldsymbol{0} & \boldsymbol{0} & 2\boldsymbol{e}_2'^T & \boldsymbol{0} \\ \boldsymbol{0} & \boldsymbol{0} & \boldsymbol{0} & \boldsymbol{0} & \boldsymbol{0} & 2\boldsymbol{e}_3'^T \\ \boldsymbol{0} & \boldsymbol{0} & \boldsymbol{0} & \boldsymbol{0} & \boldsymbol{e}_3'^T & \boldsymbol{e}_2'^T \end{bmatrix}, \quad \delta\boldsymbol{\varphi} = \begin{bmatrix} \delta\boldsymbol{u}' \\ \delta\boldsymbol{w} \\ \delta\boldsymbol{e}_2 \\ \delta\boldsymbol{e}_3 \\ \delta\boldsymbol{e}_2' \\ \delta\boldsymbol{e}_3' \end{bmatrix}. \tag{47}$$

4.3. Internal virtual work

Having derived the expressions for the admissible variations of the current basis vectors and the generalized strains we develop in this section the expressions for the internal virtual work of the beam. Recalling Eq. (31), the internal virtual work of a three dimensional body can be written in vector form as

$$G_{int}(\boldsymbol{\phi}, \delta\boldsymbol{\phi}) = \int_{\mathcal{B}_0} \delta\boldsymbol{\epsilon}^T \boldsymbol{\sigma}\, dV, \tag{48}$$

which in the curvilinear coordinate system is written as

$$G_{int}(\boldsymbol{\phi}, \delta\boldsymbol{\phi}) = \int_\ell \int_S \int_e \delta\boldsymbol{\epsilon}^T \boldsymbol{\sigma}\, dn\, ds\, dx. \tag{49}$$

We can now use the definition of the shell resultant forces in Eq. (22) to reduce the 3D formulation to a 2D formulation. Therefore, integration of Eq. (49) in the n direction we can write the internal virtual work in terms of shell quantities as

$$G_{int}(\boldsymbol{\phi}, \delta\boldsymbol{\phi}) = \int_\ell \int_S \delta\boldsymbol{\epsilon}_s^T \boldsymbol{N}_s ds\, dx. \tag{50}$$

The reduction to a one dimensional formulation is now aided by the deduction of 1D beam forces presented in Eq. (28). Transforming the virtual curvilinear shell strains into virtual generalized strains we can rewrite the last expression as

$$G_{int}(\boldsymbol{\phi}, \delta\boldsymbol{\phi}) = \int_\ell \delta\boldsymbol{\epsilon}^T \left(\int_S \mathcal{T}^T \boldsymbol{N}_s\, ds \right) dx \tag{51}$$

In which the term in parentheses is the generalized beam forces vector (see Eq. (28)). Recalling Eq. (27) the beam forces vector can be found as a function of the shell stresses as

$$\boldsymbol{S}(x) = \int_S \mathcal{T}^T \boldsymbol{N}_s\, ds. \tag{52}$$

The explicit expression of the beam forces can be found in Appendix A.1.

Finally, we write the one dimensional version of the virtual work principle in terms of the generalized strains and the generalized beam forces

$$G_{int}(\boldsymbol{\phi}, \delta\boldsymbol{\phi}) = \int_\ell \delta\boldsymbol{\varepsilon}^T \boldsymbol{S}\, dx. \tag{53}$$

4.4. External virtual work

The virtual work of external forces can be written as

$$G_{ext}(\boldsymbol{\phi}, \delta\boldsymbol{\phi}) = \int_\ell (\boldsymbol{n} \cdot \delta\boldsymbol{u} + \boldsymbol{m} \cdot \delta\boldsymbol{\theta})\, dx, \tag{54}$$

where $\boldsymbol{n}$ is the external forces vector and $\boldsymbol{m}$ the external moments vector. These vectors are defined according to

$$\begin{aligned} \boldsymbol{n} &= \int_S \int_e \boldsymbol{b}\, dn\, ds + \int_S \boldsymbol{t}\, ds, \\ \boldsymbol{m} &= \int_S \int_e \boldsymbol{X} \times \boldsymbol{b}\, dn\, ds + \int_S \boldsymbol{X} \times \boldsymbol{t}\, ds, \end{aligned} \tag{55}$$

where $\boldsymbol{b}$ is the distributed body force vector and $\boldsymbol{t}$ is external stress vector.

4.5. Weak form of equilibrium

The variational equilibrium statement can now be written in terms of generalized components of 1D forces and strains. Recalling Eqs. (53) and (54) the virtual work of a composite beam is presented in its one dimensional form as

$$G(\boldsymbol{\phi}, \delta\boldsymbol{\phi}) = \int_\ell \delta\boldsymbol{\varepsilon}^T \boldsymbol{S}\, dx - \int_\ell (\boldsymbol{n} \cdot \delta\boldsymbol{u} + \boldsymbol{m} \cdot \delta\boldsymbol{\theta}) dx. \tag{56}$$

Using Eq. (46) it is possible to re-write the last expression as

$$G(\boldsymbol{\phi}, \delta\boldsymbol{\phi}) = \int_\ell [\mathbb{H}\delta\boldsymbol{\varphi}]^T \boldsymbol{S} dx - \int_\ell \boldsymbol{n} \cdot \delta\boldsymbol{u} + \boldsymbol{m} \cdot \delta\boldsymbol{\theta} dx. \tag{57}$$

5. Linearization of the weak form

The solution of the nonlinear system of equations requires the linearization of these equations with respect to an increment in the configurations variables. The linearization of the variational equilibrium equations is obtained through the directional derivative and, assuming conservative loading, its application gives two tangent terms; the material and the geometric stiffness matrices.

Being $L[G(\boldsymbol{\phi}, \delta\boldsymbol{\phi})]$ the linear part of the functional $G(\boldsymbol{\phi}, \delta\boldsymbol{\phi})$, we have

$$L[G(\hat{\boldsymbol{\phi}}, \delta\boldsymbol{\phi})] = G(\hat{\boldsymbol{\phi}}, \delta\boldsymbol{\phi}) + DG(\hat{\boldsymbol{\phi}}, \boldsymbol{\delta}\phi) \cdot \Delta\boldsymbol{\phi}, \tag{58}$$

where the first term $G(\hat{\boldsymbol{\phi}}, \boldsymbol{\delta}\phi)$ is the unbalanced force at the configuration $\hat{\boldsymbol{\phi}}$ (for simplicity, the hat operator $\widehat{\ }$ will be omitted hereafter). The Frechet differential in the second term is

obtained in a standard way as

$$DG(\boldsymbol{\phi},\delta\boldsymbol{\phi})\cdot\Delta\boldsymbol{\phi}=\frac{d}{d\epsilon}G(\boldsymbol{\phi}+\epsilon\Delta\boldsymbol{\phi})\big|_{\epsilon=0}, \tag{59}$$

where $\Delta\boldsymbol{\phi}$ fulfills the geometric boundary conditions. For simplicity, we have dropped $\widehat{\ }$. Applying the definition in Eq. (59) and recalling Eqs. (53) and (45), we obtain the tangent stiffness as

$$DG_{int}(\boldsymbol{\phi},\boldsymbol{\delta}\phi)\cdot\Delta\boldsymbol{\phi}=\int_{\ell}(\delta\boldsymbol{\varepsilon}^T\mathbb{D}\Delta\boldsymbol{\varepsilon}+\Delta\delta\boldsymbol{\varepsilon}^T\boldsymbol{S})dx, \tag{60}$$

where ℓ is the length of the undeformed beam. The integral of the first term gives raise to the material stiffness matrix and from the integral of the second term evolves the geometric stiffness matrix.

Using Eq. (46) the first term of the above equation takes the form

$$D_1G_{int}(\boldsymbol{\phi},\delta\boldsymbol{\phi})\cdot\Delta\boldsymbol{\phi}=\int_{\ell}\delta\boldsymbol{\varphi}^T\mathbb{H}^T\mathbb{D}\mathbb{H}\Delta\boldsymbol{\varphi}\,dx. \tag{61}$$

On the other hand, from Eq. (59); the general expression of the geometric stiffness operator gives

$$D_2G_{int}(\boldsymbol{\phi},\delta\boldsymbol{\phi})\cdot\Delta\boldsymbol{\phi}=\int_{\ell}\Delta\delta\boldsymbol{\varepsilon}^T\boldsymbol{S}\,dx. \tag{62}$$

The linearization of the virtual generalized strains gives

$$\Delta\delta\boldsymbol{\varepsilon}=\begin{bmatrix}\delta\boldsymbol{u}'\cdot\Delta\boldsymbol{u}'\\ \delta\boldsymbol{u}'\cdot\Delta\boldsymbol{e}_3'+\delta\boldsymbol{e}_3'\cdot\Delta\boldsymbol{u}'+\boldsymbol{x}_0'\cdot\Delta\delta\boldsymbol{e}_3'\\ \delta\boldsymbol{u}'\cdot\Delta\boldsymbol{e}_2'+\delta\boldsymbol{e}_2'\cdot\Delta\boldsymbol{u}'+\boldsymbol{x}_0'\cdot\Delta\delta\boldsymbol{e}_2'\\ \delta\boldsymbol{u}'\cdot\Delta\boldsymbol{e}_2+\delta\boldsymbol{e}_2\cdot\Delta\boldsymbol{u}'+\boldsymbol{x}_0'\cdot\Delta\delta\boldsymbol{e}_2\\ \delta\boldsymbol{u}'\cdot\Delta\boldsymbol{e}_3+\delta\boldsymbol{e}_3\cdot\Delta\boldsymbol{u}'+\boldsymbol{x}_0'\cdot\Delta\delta\boldsymbol{e}_3\\ \delta\boldsymbol{e}_2'\cdot\Delta\boldsymbol{e}_3+\delta\boldsymbol{e}_3\cdot\Delta\boldsymbol{e}_2'+\boldsymbol{e}_3\cdot\Delta\delta\boldsymbol{e}_2'+\boldsymbol{e}_2'\cdot\Delta\delta\boldsymbol{e}_3\\ 2(\boldsymbol{e}_2'\cdot\Delta\delta\boldsymbol{e}_2'+\delta\boldsymbol{e}_2'\cdot\Delta\boldsymbol{e}_2')\\ 2(\boldsymbol{e}_3'\cdot\Delta\delta\boldsymbol{e}_3'+\delta\boldsymbol{e}_3'\cdot\Delta\boldsymbol{e}_3')\\ \delta\boldsymbol{e}_2'\cdot\Delta\boldsymbol{e}_3'+\delta\boldsymbol{e}_3'\cdot\Delta\boldsymbol{e}_2'+\boldsymbol{e}_3'\cdot\Delta\delta\boldsymbol{e}_2'+\boldsymbol{e}_2'\cdot\Delta\delta\boldsymbol{e}_3'\end{bmatrix} \tag{63}$$

To complete the development of the geometric stiffness matrix we need to find the linearization of the virtual generalized strains $\Delta\delta\boldsymbol{\varepsilon}^T$, but we first need to obtain the linearized virtual directors. Using Eq. (42), the linearization of the virtual directors can be obtained as

$$\Delta\delta\boldsymbol{e}_i=(\Delta\boldsymbol{T}\delta\boldsymbol{\theta})\times\boldsymbol{e}_i+(\boldsymbol{T}\delta\boldsymbol{\theta})\times[(\boldsymbol{T}\Delta\boldsymbol{\theta})\times\boldsymbol{e}_i]. \tag{64}$$

The linearization of the virtual director derivatives is more involved, it has a complicated expression that requires the linearization of both the tangential map ($\Delta\boldsymbol{T}$) and its variation ($\Delta\delta\boldsymbol{T}$). By recalling Eq. (44) we obtain

$$\begin{aligned}\Delta\delta\boldsymbol{e}_i'&=\Delta(\delta T\boldsymbol{\theta}'+\boldsymbol{T}\delta\boldsymbol{\theta}')\times\boldsymbol{e}_i+(\delta T\boldsymbol{\theta}'+\boldsymbol{T}\delta\boldsymbol{\theta}')\times\Delta\boldsymbol{e}_i+\Delta(T\boldsymbol{\theta}')\\&\quad\times[(\boldsymbol{T}\delta\boldsymbol{\theta})\times\boldsymbol{e}_i]+(T\boldsymbol{\theta}')\times\Delta[(\boldsymbol{T}\delta\boldsymbol{\theta})\times\boldsymbol{e}_i]\\&=[(\Delta\delta T\boldsymbol{\theta}'+\delta\boldsymbol{T}\Delta\boldsymbol{\theta}')+(\Delta\boldsymbol{T}\delta\boldsymbol{\theta}'+\boldsymbol{T}\Delta\delta\boldsymbol{\theta}')]\times\boldsymbol{e}_i+(\delta T\boldsymbol{\theta}'+\boldsymbol{T}\delta\boldsymbol{\theta}')\\&\quad\times\Delta\boldsymbol{e}_i+(\Delta T\boldsymbol{\theta}'+\boldsymbol{T}\Delta\boldsymbol{\theta}')\times[(\boldsymbol{T}\delta\boldsymbol{\theta})\times\boldsymbol{e}_i]+(T\boldsymbol{\theta}')\\&\quad\times[(\Delta\boldsymbol{T}\delta\boldsymbol{\theta})\times\boldsymbol{e}_i+(\boldsymbol{T}\delta\boldsymbol{\theta})\times\Delta\boldsymbol{e}_i]\end{aligned} \tag{65}$$

To find $\Delta\delta\boldsymbol{\varepsilon}$ in terms of the kinematic variables we would need to inject the expressions in Eqs. (64) and (65) into Eq. (63). As it will be clarified in the next section; in order to avoid the use of such complicated expression for $\Delta\delta\boldsymbol{e}_i'$, we will use interpolation of $\Delta\delta\boldsymbol{e}_i$ to obtain the discrete form of Eq. (63). So, the geometric stiffness matrix will be directly formulated in its discrete form.

6. Finite element formulation

The implementation of the proposed finite element is based on linear interpolation and one point reduced integration (thus avoiding shear locking). The most relevant procedure of the finite element implementation is the use of interpolation to obtain the derivatives of the director field, this greatly simplifies the expression of the tangent matrix.

6.1. Interpolations and directors update

We interpolate the position vectors in the undeformed and deformed configuration as

$$\boldsymbol{X}=\sum_{j=1}^{nn}N_j\hat{\boldsymbol{X}}_j,\quad \boldsymbol{x}=\sum_{j=1}^{nn}N_j(\hat{\boldsymbol{X}}_j+\hat{\boldsymbol{u}}_j), \tag{66}$$

where $\widehat{\ }$ will hereon indicate nodal values, N_j is the shape function value at node j and nn is the number of nodes per element (which in the present case is 2). Using Eq. (1) the director field at the iteration $n+1$ is found as

$$^{n+1}\boldsymbol{e}_i=\boldsymbol{\Lambda}(^{n+1}\boldsymbol{\theta})\boldsymbol{E}_i, \tag{67}$$

where $\boldsymbol{\Lambda}$ is the *total rotation tensor*.

According to Eq. (67), we could find the derivative of the directors as

$$\boldsymbol{e}_i'=\boldsymbol{\Lambda}'\boldsymbol{E}_i \tag{68}$$

as done in most Total Lagrangian formulations [6,21]; but this greatly complicates the expression for the variation of the derivative of the directors and also requires the calculation of the derivative of the rotation tensor. As a consequence, the linearization process is cumbersome and the resulting expressions of the tangent stiffness matrices are much more complicated. In order to simplify the derivation we use interpolation to obtain the directors derivatives. So, it will be accepted that

$$\boldsymbol{e}_i'\cong\sum_{j=1}^{nn}N_j'\hat{\boldsymbol{e}}_i^j \tag{69}$$

where $\hat{\boldsymbol{e}}_i^j$ stands for the director i at the node j. Although this approximation is expected to be accurate enough to be used in almost every practical situation, we will analyze in the numerical investigations section the impact of this approximation in the accuracy of the solution. As it will be shown later, the use of interpolation to obtain the derivative of the director field leads to a path independent solution.

6.2. Objectivity of the generalized strain measures

Several works have been devoted to demonstrate the preservation of the objectivity of the discrete strain measures [13–20]. The works of Crisfield and Jelenic [13,14] shown that geometrically exact beam finite element formulations parametrized with iterative spins, incremental rotation vectors and total rotation vector fail to satisfy the objectivity of its discrete strain measures. Recently, Mäkinen [21] showed that their conclusions regarding the objectivity of the discrete strain measures of formulations parametrized with the total and the incremental rotation vector are incorrect. The misleading conclusions in [13,14] about the Total and Updated Lagrangian formulations arise from the fact that linear interpolation does not preserve an observer transformation, which in the cited work was assumed.

In virtue of the desire of obtaining a formulation where the discrete strain measures are objective, interesting works presented formulations that gained that property by avoiding the interpolation of rotation variables [16–18]. This was aided by parametrizing the equation of motion in terms of nodal triads, obtaining the discrete forms via interpolation of directors. Although the discrete strain measures derived in this works preserve the objectivity property, the linearization of the spins was not consistent and the tangent stiffness matrix results to be non-symmetrical (implying the loss of the quadratic convergence property).

In the present formulation we have chosen a mixed approach, parametrizing the finite rotations with the total rotation vector and the strain measures with the directors and its derivatives. It is interesting note that the parametrization of the variational formulation with the directors greatly simplifies the expressions of the tangent stiffness matrix (as it is showed in next Section 6.3). However, the linearization of the director variation cannot be written exclusively in terms of directors and it is not possible to fully eliminate interpolated rotations from the formulation. The "propagation" of interpolated rotations shall clearly be seen from the expression of the matrix $\mathbb{B}$.

To check the objectivity of the generalized discrete strain measures we superpose a rigid body motion to the configuration and then test the invariance of the strains. The rigid body motion modifies the current configuration as

$$\boldsymbol{x}_0^* = \boldsymbol{c} + \boldsymbol{Q}\boldsymbol{x}_0 \quad \boldsymbol{e}_i^* = \boldsymbol{Q}\boldsymbol{e}_i \tag{70}$$

where $\boldsymbol{c} \in \mathbb{R}^3$ and $\boldsymbol{Q} \in \mathrm{SO}(3)$. If, for simplicity, we assume zero initial strain and we apply the above transformations to Eq. (10) and consider, for example, its effect over κ_2 we have

$$\begin{aligned}
\kappa_2 &= \left(\sum_{j=1}^{nn} N_j' \boldsymbol{x}_0^j\right) \cdot \left(\sum_{j=1}^{nn} N_j' \hat{\boldsymbol{e}}_3^j\right) \\
\kappa_2^* &= \left[\boldsymbol{c} + \boldsymbol{Q}\left(\sum_{j=1}^{nn} N_j \boldsymbol{x}_0^j\right)\right]' \cdot \left[\boldsymbol{Q}\left(\sum_{j=1}^{nn} N_j \hat{\boldsymbol{e}}_3^j\right)\right]' \\
&= \left[\boldsymbol{c}' + \boldsymbol{Q}'\left(\sum_{j=1}^{nn} N_j \boldsymbol{x}_0^j\right) + \boldsymbol{Q}\left(\sum_{j=1}^{nn} N_j' \boldsymbol{x}_0^j\right)\right] \cdot \left(\boldsymbol{Q}' \sum_{j=1}^{nn} N_j \hat{\boldsymbol{e}}_3^j + \boldsymbol{Q} \sum_{j=1}^{nn} N_j' \hat{\boldsymbol{e}}_3^j\right)
\end{aligned} \tag{71}$$

Noting that since the rigid body motion is fixed $\boldsymbol{c}' = \boldsymbol{Q}' = 0$, we have

$$\kappa_2^* = \boldsymbol{Q}\left(\sum_{j=1}^{nn} N_j' \boldsymbol{x}_0^j\right) \cdot \left(\boldsymbol{Q} \sum_{j=1}^{nn} N_j' \hat{\boldsymbol{e}}_3^j\right) = \left(\sum_{j=1}^{nn} N_j' \boldsymbol{x}_0^j\right) \cdot \left(\boldsymbol{Q}^T\boldsymbol{Q} \sum_{j=1}^{nn} N_j' \hat{\boldsymbol{e}}_3^j\right) \tag{72}$$

Now, the orthogonality property of the superimposed rotation gives $\boldsymbol{Q}^T\boldsymbol{Q} = I$, and thus

$$\kappa_2^* = \kappa_2 = \left(\sum_{j=1}^{nn} N_j' \boldsymbol{x}_0^j\right) \cdot \left(\sum_{j=1}^{nn} N_j' \hat{\boldsymbol{e}}_3^j\right) \tag{73}$$

From which we observe that the generalized strain measure is not affected by the superimposed rigid body motion. It is interesting to note that since linear interpolation of vector fields is invariant under rigid body motion (i.e. $\boldsymbol{Q}\sum_{j=1}^{nn} N_j' \hat{\boldsymbol{e}}_i^j = \sum_{j=1}^{nn} N_j' (\boldsymbol{Q}\hat{\boldsymbol{e}}_i^j)$) and the scalar product is invariant under orthogonal transformations, the above conclusion clearly makes sense. The frame invariance of the remaining generalized strains can be proven in a similar manner. We note that the generalized strains can be obtained by interpolation of nodal strains as $\kappa_2 = \sum_{j=1}^{nn} N_j'(\boldsymbol{x}_{0j} \cdot \hat{\boldsymbol{e}}_i^j)$, But although the frame invariance property is maintained, this form of calculating the discrete strains is less accurate.

6.3. Discrete virtual directors

The objective of this section is to obtain the discrete version of the virtual generalized strains and its linearization; first we need to obtain the discrete version of the director variation and its derivatives. Regarding the director variations, although the expression in Eq. (44) does not complicate substantially the formulation, expression (65) actually does. A simpler way to obtain the director variations would help to simplify the expression of the tangent stiffness very much.

Assuming holonomic constraints we may interchange variations and derivatives, i.e. $\delta(\boldsymbol{e}') = (\delta\boldsymbol{e})'$. Using this property, we can use Eq. (69) to obtain the variation of the directors and its derivatives as

$$\delta\boldsymbol{e}_i \cong \sum_{j=1}^{nn} N_j \delta\hat{\boldsymbol{e}}_i^j, \quad \delta\boldsymbol{e}_i' \cong \sum_{j=1}^{nn} N_j' \delta\hat{\boldsymbol{e}}_i^j, \tag{74}$$

The obtention of the linearization of the directors and its derivatives is more involved and requires the linearization of the tangential transformation defined in Eq. (39). Observing the linearization of the variation of the directors appears in the virtual strains (and also in its linearization) always pre multiplied by some constant vector $\boldsymbol{a}$, it is preferable to obtain the expression for this product and not only for the second variation. Thus, recalling Eq. (64) we find that

$$\boldsymbol{a} \cdot \Delta\delta\boldsymbol{e}_i = \boldsymbol{a} \cdot \{(\Delta\boldsymbol{T}\delta\boldsymbol{\theta}) \times \boldsymbol{e}_i + (\boldsymbol{T}\delta\boldsymbol{\theta}) \times [(\boldsymbol{T}\Delta\boldsymbol{\theta}) \times \boldsymbol{e}_i]\} \tag{75}$$

Switching to matrix notation, using spinors in place of cross products and reordering some terms we can re-write the above equation as

$$\boldsymbol{a} \cdot \Delta\delta\boldsymbol{e}_i = \delta\boldsymbol{\theta}^T \Delta\boldsymbol{T}^T(\tilde{\boldsymbol{e}}_i\boldsymbol{a}) + \delta\boldsymbol{w}^T(\tilde{\boldsymbol{a}}\tilde{\boldsymbol{e}}_i)\Delta\boldsymbol{w}, \tag{76}$$

where $\tilde{\boldsymbol{e}}_i$ is the spinor of the director i and

$$\Delta\boldsymbol{T}^T(\tilde{\boldsymbol{e}}_i\boldsymbol{a}) = D[\boldsymbol{T}^T(\tilde{\boldsymbol{e}}_i\boldsymbol{a})] \cdot \Delta\boldsymbol{\theta}. \tag{77}$$

The linearization of the term $\boldsymbol{T}^T(\tilde{\boldsymbol{e}}_i\boldsymbol{a})$ gives

$$\begin{aligned}
D[\boldsymbol{T}^T(\tilde{\boldsymbol{e}}_i\boldsymbol{a})] \cdot \Delta\boldsymbol{\theta} = \{&c_1\boldsymbol{a} \otimes \boldsymbol{\theta} - c_2(\tilde{\boldsymbol{\theta}}a) \otimes \boldsymbol{\theta} + c_3(\boldsymbol{\theta} \cdot \boldsymbol{a})\boldsymbol{\theta} \otimes \boldsymbol{\theta} - c_4\tilde{\boldsymbol{a}} \\
&+ c_5[(\boldsymbol{\theta} \cdot \boldsymbol{a})\boldsymbol{I} + \boldsymbol{\theta} \otimes \boldsymbol{a}]\} \cdot \Delta\boldsymbol{\theta}.
\end{aligned} \tag{78}$$

where

$$\begin{aligned}
&c_1 = \frac{\theta\cos\theta - \sin\theta}{\theta^3}, \quad c_2 = \frac{\theta\sin\theta + 2\cos\theta - 2}{\theta^4}, \\
&c_3 = \frac{3\sin\theta - 2\theta - \theta\cos\theta}{\theta^5}, \quad c_4 = \frac{\cos\theta - 1}{\theta^2}, \quad c_3 = \frac{\theta - \sin\theta}{\theta^3}
\end{aligned} \tag{79}$$

Now, introducing Eq. (78) into Eq. (76) and recalling Eq. (38) it is possible to rewrite the discrete form of Eq. (76) as

$$\boldsymbol{a} \cdot \Delta\delta\boldsymbol{e}_i \cong \delta\hat{\boldsymbol{w}}^T \left[\sum_{j=1}^{nn} N_j[\Xi(\boldsymbol{a}, \hat{\boldsymbol{e}}_i^j) + \tilde{\boldsymbol{a}}\tilde{\hat{\boldsymbol{e}}}_i^j]\right] \Delta\hat{\boldsymbol{w}}, \tag{80}$$

where $\tilde{\hat{\boldsymbol{e}}}_i^j$ is the spinor of the director i at node j and

$$\Xi(\boldsymbol{a}, \hat{\boldsymbol{e}}_i^j) = \boldsymbol{T}^{-1T}(D[\boldsymbol{T}^T(\tilde{\boldsymbol{e}}_i\boldsymbol{a})] \cdot \Delta\boldsymbol{\theta})\boldsymbol{T}^{-1}. \tag{81}$$

In the same form, the expression for the second variation of the director's derivatives can be found in its discrete form by making use of Eq. (74)

$$\boldsymbol{a} \cdot \Delta\delta\boldsymbol{e}_i' = \delta\hat{\boldsymbol{w}}^T \left[\sum_{j=1}^{nn} N_j'[\Xi(\boldsymbol{a}, \hat{\boldsymbol{e}}_i^j) + \tilde{\boldsymbol{a}}\tilde{\hat{\boldsymbol{e}}}_i^j]\right] \Delta\hat{\boldsymbol{w}} \tag{82}$$

The last expressions show that consistent linearization of virtual directors necessarily leads to terms that are conjugate to rotations. This precludes the possibility of obtaining a consistent tangent stiffness free of interpolated rotations.

6.4. Discrete virtual strains

Having derived the expressions for the discrete virtual directors, its derivatives and its corresponding linearization, it is now possible to find a discrete expression for the discrete virtual generalized strain and its linearization.

We can relate the two kinematic vectors $\delta\boldsymbol{\varphi}$ and $\delta\boldsymbol{\phi}$ by means of a matrix $\mathbb{B}$ as

$$\delta\boldsymbol{\varphi} \cong \sum_{j=1}^{nn} \mathbb{B}_j \delta\hat{\boldsymbol{\phi}}_j, \tag{83}$$

where

$$\mathbb{B}_j = \begin{bmatrix} \boldsymbol{N}_j' & \boldsymbol{0} \\ \boldsymbol{0} & N_j \boldsymbol{T}_j \\ 0 & N_j \tilde{\boldsymbol{e}}_2^{jT} \boldsymbol{T}_j \\ 0 & N_j \tilde{\boldsymbol{e}}_3^{jT} \boldsymbol{T}_j \\ 0 & N_j' \tilde{\boldsymbol{e}}_2^{jT} \boldsymbol{T}_j \\ 0 & N_j' \tilde{\boldsymbol{e}}_3^{jT} \boldsymbol{T}_j \end{bmatrix}, \quad \delta\hat{\boldsymbol{\phi}}_j = \begin{bmatrix} \delta\hat{\boldsymbol{u}}_j \\ \delta\hat{\boldsymbol{\theta}}_j \end{bmatrix} \cdot \begin{bmatrix} \delta\boldsymbol{u}' \\ \delta\boldsymbol{w} \\ \delta\boldsymbol{e}_2 \\ \delta\boldsymbol{e}_3 \\ \delta\boldsymbol{e}_2' \\ \delta\boldsymbol{e}_3' \end{bmatrix} \tag{84}$$

where $\tilde{\ }$ indicates the skew symmetric matrix of a vector, $\hat{\ }$ indicates a nodal variable. Thus $\tilde{\boldsymbol{e}}_i^j$ is a skew director in the direction i of the node j and $\boldsymbol{T}_j$ is a tangential transformation at this node. Henceforth summation over index j will be implicitly defined, so we will omit the summation symbol and the node index i.

Finally, recalling Eq. (46) we can write the virtual generalized strains as

$$\delta\boldsymbol{\varepsilon} \cong \mathbb{H}\mathbb{B}\delta\hat{\boldsymbol{\phi}}. \tag{85}$$

The discrete form of the incremental virtual strains, i.e. $\Delta\delta\boldsymbol{\varepsilon}$, is more difficult to obtain. Using the structure of the geometric stiffness operator of Eq. (62) we can obtain a matrix $\mathbb{G}$ as to satisfy the equality $\Delta\delta\boldsymbol{\varepsilon}^T\boldsymbol{S} = \delta\boldsymbol{\varphi}^T\mathbb{G}\Delta\boldsymbol{\varphi}$, a lengthy manipulation gives

$$\mathbb{G} = \begin{bmatrix} \overline{S}_1 & \boldsymbol{0} & \overline{Q}_2 & \overline{Q}_3 & \overline{M}_3 & \overline{M}_2 \\ & \boldsymbol{A} & \boldsymbol{0} & \boldsymbol{0} & \boldsymbol{0} & \boldsymbol{0} \\ & & \boldsymbol{0} & \boldsymbol{0} & \boldsymbol{0} & \boldsymbol{0} \\ & & & \boldsymbol{0} & \overline{M}_1 & \boldsymbol{0} \\ & Sym & & & 2\overline{P}_2 & \overline{P}_{23} \\ & & & & & 2\overline{P}_3 \end{bmatrix}. \tag{86}$$

where

$$\begin{aligned} \boldsymbol{A} = \sum_{j=1}^{2} \{ & (M_2 N_j' + Q_3 N_j)[\Xi(\boldsymbol{x}_0', \hat{\boldsymbol{e}}_3^j) + \tilde{\boldsymbol{x}}_0' \tilde{\boldsymbol{e}}_3^j] \\ & + (M_3 N_j' + Q_2 N_j)[\Xi(\boldsymbol{x}_0', \hat{\boldsymbol{e}}_2^j) + \tilde{\boldsymbol{x}}_0' \tilde{\boldsymbol{e}}_2^j] \\ & + T[N_j'[\Xi(\boldsymbol{e}_3, \hat{\boldsymbol{e}}_2^j) + \tilde{\boldsymbol{e}}_3 \tilde{\boldsymbol{e}}_2^j] + N_j[\Xi(\boldsymbol{e}_2', \hat{\boldsymbol{e}}_3^j) + \tilde{\boldsymbol{e}}_2' \tilde{\boldsymbol{e}}_3^j]] \\ & + 2P_2 N_j'[\Xi(\boldsymbol{e}_2', \hat{\boldsymbol{e}}_2^j) + \tilde{\boldsymbol{e}}_2' \tilde{\boldsymbol{e}}_2^j] + 2P_3 N_j'[\Xi(\boldsymbol{e}_3', \hat{\boldsymbol{e}}_3^j) + \tilde{\boldsymbol{e}}_3' \tilde{\boldsymbol{e}}_3^j] \\ & + P_{23}[N_j'[\Xi(\boldsymbol{e}_3', \hat{\boldsymbol{e}}_2^j) + \tilde{\boldsymbol{e}}_3' \tilde{\boldsymbol{e}}_2^j] + N_j'[\Xi(\boldsymbol{e}_2', \hat{\boldsymbol{e}}_3^j) + \tilde{\boldsymbol{e}}_2' \tilde{\boldsymbol{e}}_3^j]] \} \end{aligned} \tag{87}$$

We note that $\boldsymbol{A}$ result to be symmetric and as a consequence $\mathbb{G}$ is also symmetric. Although it is strictly not a necessary condition, the fact that the matrix $\mathbb{G}$ is symmetric, guarantees the symmetry of the tangent stiffness matrix.

6.5. Tangent stiffness matrix

Introducing Eq. (83) into Eq. (61) we can obtain the discrete form of the material virtual work as

$$D_1 G_{int}(\hat{\boldsymbol{\phi}}, \delta\hat{\boldsymbol{\phi}}) \cdot \Delta\hat{\phi} = \int_\ell (\mathbb{B}\delta\hat{\boldsymbol{\phi}})^T \mathbb{H}^T \mathbb{D}\mathbb{H}(\mathbb{B}\Delta\hat{\boldsymbol{\phi}}) dx. \tag{88}$$

Then, the element material stiffness matrix is

$$\boldsymbol{k}_M = \int_\ell \mathbb{B}^T \mathbb{H}^T \mathbb{D}\mathbb{H}\mathbb{B} dx. \tag{89}$$

Proceeding in a similar way, we use Eqs. (86) and (62) to obtain the discrete geometric stiffness terms as

$$D_2 G_{int}(\hat{\boldsymbol{\phi}}, \delta\hat{\boldsymbol{\phi}}) \cdot \Delta\hat{\boldsymbol{\phi}} = \int_\ell (\mathbb{B}\delta\hat{\boldsymbol{\phi}})^T \mathbb{G}(\mathbb{B}\Delta\hat{\boldsymbol{\phi}}) dx. \tag{90}$$

Therefore, the element geometric stiffness matrix becomes

$$\boldsymbol{k}_G = \int_\ell \mathbb{B}^T \mathbb{G}\mathbb{B} dx. \tag{91}$$

Following the standard steps of the finite element method, the element and global tangent stiffness matrices are

$$\begin{aligned} \boldsymbol{k}_T &= \int_\ell \mathbb{B}^T (\mathbb{H}^T \mathbb{D}\mathbb{H} + \mathbb{G}) \mathbb{B} dx, \\ \boldsymbol{K}_T &= \sum_{e=1}^{els} \boldsymbol{k}_T, \end{aligned} \tag{92}$$

where the summation operator is used to represent the finite element assembly process.

7. Numerical investigations

In this section we show the behavior of the proposed beam element using different benchmark tests proposed in the literature. Most of existing geometrically exact finite elements cannot deal with composite materials, so in tests involving composite materials the proposed finite element is compared against 3D shell models and the formulation presented in [28]. The shell models were built with Abaqus S4R elements and contain an average of 50,000 DOF. In order to test the proposed finite elements against other reported formulations [4,40], we set the material to be isotropic. The results presented for the formulations [4,40] were obtained using the research software FEAP [41]

7.1. Accuracy assessment 1—roll up of a cantilever beam

In the first test we choose a classical pure bending test; the roll up of a cantilever beam, to test the behavior of the formulation in extreme deformation cases. We use an isotropic material to compare the formulation against other reported geometrically exact beam finite element formulations.

The tested specimen is a thin-walled beam with a square cross section ($b=0.5$, $h=0.5$ and $t=0.05$) and a length of 50. The material constants are: $E=144\times10^9$ and $\nu=0.3$. With the Euler formula: $\theta = Ml/EI$ we obtain the magnitude of the two moments that, applied at the tip of the beam, produce a deformed shape of half a circle and a full circle of a Bernoulli–Euler beam, respectively. These moments are: $M_1=3.80761\times10^7$ and $M_2=7.615221\times10^7$. Fig. 4 shows the deformed shapes obtained after application of these moments.

Tables 1 and 2 present the numerical results obtained for the maximum tip displacements for both load cases (M_1 and M_2).

As it can be observed from Tables 1 and 2, the present finite element has a relatively poor performance when the mesh is coarse. This is an expected behavior since the obtention of the derivatives of the director field using interpolation introduces and additional interpolation error that the formulations based on the derivative of the rotation tensor does not have. However, it is clearly seen that increasing the number of elements the solution converges to the solution presented in [28]. Thus, convergence of the proposed finite element can simply be adjusted by increasing the mesh density.

It should be noted that for the present example the Eulerian formulation and a Total Lagrangian formulation that does not use directors interpolation should give the same results, except for

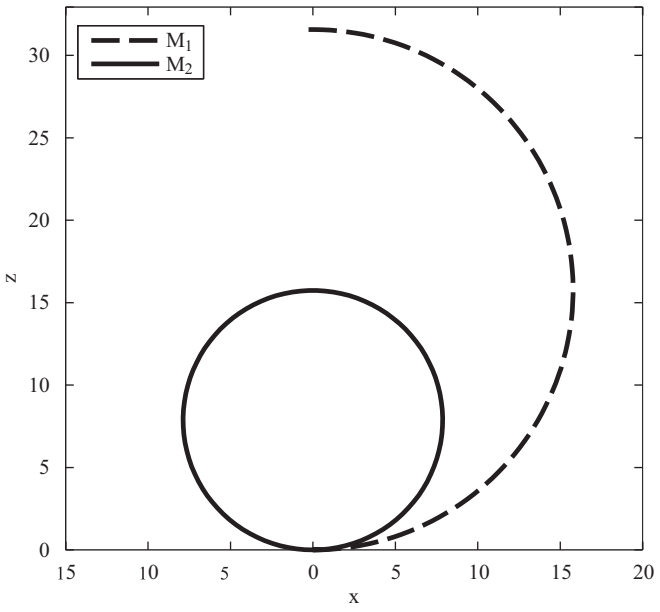

Fig. 4. Roll up test.

Table 1
Displacements components for M_1.

	Tip vertical displacement	Tip horizontal displacement	Max vertical displacement	Elements
Simo and Vu-Quoc (FEAP)	31.673 31.546	−50.448 −50.446	31.673 31.546	10 50
Ibrahimbegovic-Al Mikad (FEAP)	31.673 31.546	−50.448 −50.446	31.673 31.546	10 50
Analytic	31.831	−50.000	31.831	–
Saravia et al. [28]	31.694 31.567	−50.405 −50.403	31.694 31.567	10 50
Present	31.108 31.554	−51.258 −50.422	31.108 31.553	10 50

Table 2
Displacements components for M_2.

	Tip vertical displacement	Tip horizontal displacement	Max vertical displacement	Elements
Simo and Vu-Quoc (FEAP)	0.013 0.012	−49.545 −49.554	16.038 15.781	10 50
Ibrahimbegovic-Al Mikad (FEAP)	0.013 0.012	−49.545 −49.554	16.038 15.781	10 50
Analytic	0.000	−50.000	15.915	–
Saravia et al. [28]	0.016 0.015	−49.494 −49.50	16.004 15.752	10 50
Present	1.263 0.024	−45.863 −49.380	14.495 15.707	10 50

the small frame invariance and path independence errors arising in the Eulerian formulation in [28].

It also important to point out that the present formulation results to be slower than the non-consistent Eulerian formulation [28], not only because it requires the computation of tangential map at the nodes but also because it is necessary to compute the linearization of the tangential map, which results to be very time consuming.

7.2. Accuracy assessment 2—pure bending of a cantilever beam

We test in this example the behavior of the accuracy of the present formulation in a full three dimensional problem where the deformation is again large. The curved beam's reference configuration given is a 45° circular segment with radius $R=100$ and lying in the x–y plane (see. Fig. 5), the beam is loaded with a vertical load (z direction). The properties of the isotropic material are: $E=1.0\times10^7$ and $v=0.3$. The cross section is a box with $b=1$, $h=1$ and $t=0.1$.

Table 3 shows the results of the bending test for $P=100$. We have used an Abaqus 3D shell model as the reference model. As it can be seen, the present finite element formulation behaves better than to the Simo and Vu-Quoc element [4] available in FEAP and the Abaqus B31 beam element. The results obtained with the present implementation and the path dependent implementation [28] are essentially the same.

The solution was reached in 5 load steps using an average of 8 iterations per step.

Increasing the load to $P=400$ we obtain also very good results (see Table 4). Note that we added to the comparison the Abaqus parabolic beam element B32. The present finite element represents the kinematic behavior of the beam very well.

7.3. Anisotropic case—pure bending of a cantilever beam

In this example we present a comparison of the displacement path of the beam using an anisotropic material, we analyze the 45° arc of Fig. 5 laminated with a $\{45,-45,-45,45\}$ configuration. The laminas are made of E-Glass fibers and an Epoxy matrix [32],

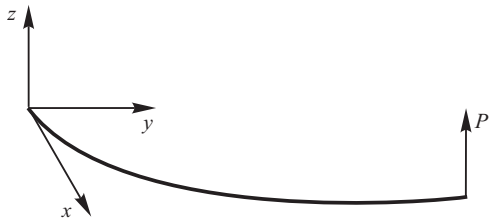

Fig. 5. Bending of a 45° arc.

Table 3
Maximum displacements in a 45° arc bending test ($P=100$).

	Tip y displacement	Tip x displacement	Tip z displacement	Elements
Abaqus Shell	−2.090	−3.641	22.611	–
Abaqus B31	−2.574	−3.570	22.734	50
Simo and Vu-Quoc (FEAP)	−1.986	−3.325	22.001	50
Saravia et. al. [28]	−2.068	−3.495	22.366	50
Present	−2.069	−3.449	22.367	50

Table 4
Maximum displacements in a 45° arc bending test ($P=400$).

	Tip y displacement	Tip x displacement	Tip z displacement	Elements
Abaqus Shell	−12.201	−21.546	50.997	–
Abaqus B31	−12.401	−21.311	−51.110	50
Abaqus B32	−12.416	−21.310	−51.111	50
Simo and Vu-Quoc (FEAP)	−12.008	−20.692	50.067	50
Saravia et. al. [28]	−12.205	−21.015	50.880	50
Present	−12.206	−21.019	50.884	50

the material properties are given in Table 5. The cross section is a box with $b=1$, $h=1$ and $t=0.1$.

To increase the complexity of the stress state in the beam we modify the applied load to have components $P_x=4.0\times10^5$, $P_y=-4.0\times10^5$, $P_z=8.0\times10^5$. Fig. 6 presents the curves that describe the evolution of the centroidal displacements along the load path (LPF being the Load Proportional Factor) in the tip of the beam and in the middle of the beam (t and m sub indexes, respectively).

It can be seen from Fig. 6 that the correlation of the present formulation against the Abaqus shell model is excellent. As expected, the present formulation gives the same results than [28]. This is a very good result since in contrast to [28]; the present formulation is frame invariant and path independent (as it will be shown in the next examples).

7.4. Anisotropic beam path independence test

We test in this example the path independence property of the proposed formulation. Using the same anisotropic curved beam of the previous example we apply a load $P=(P_x,P_y,P_z)$ in six steps and analyze the resulting displacements at the ending of the load cycle. The loading scheme is shown in Table 6, it must be noted that the load on each step is propagated to the following step. Since the load at the end of the last step is zero in a path independent formulation the resulting displacements must also be zero.

As Table 7 shows, the present finite element is path independent, both the displacements and rotations come back to zero after retiring the load. Also, it can be observed that this property is independent of both the incremental scheme and the number of elements.

7.5. Anisotropic beam frame invariance test

This example is very similar to that proposed in Crisfield and Jelenic [13], it is used to show the frame-invariance of the finite element formulation. It consist on an L-shaped frame lying in the x–y plane that is first loaded with a tip force $\boldsymbol{F}$ and then rotated around the x, y and z axes. The frame has a leg lying in the x axis with a length of 10 and a leg parallel to the y axis with a length of 5. The cross section is boxed with dimensions $h=1$, $b=1$ and a thickness of 0.1; and is made of 4 layers of E-Glass Fiber-Epoxy, laminated in a $\{45,-45,-45,45\}$ configuration. The material properties are given in Table 5.

The first load case consist on a tip force of 2×10^7, fixed in the z direction; the second load is applied in three different ways: (i) rotation around the z axis, (ii) rotation around the y axis and (iii) rotation around the x axis. For both i, ii, and iii the rotation is imposed in 4000 increments of $\pi/20$ rad each, which is equivalent to 100 revolutions.

Fig. 7 shows the evolution of displacements after completing each revolution; as expected from a frame-indifferent formulation, the displacements remain constant along the revolutions. Since the constant displacements are the result of the first load case and we have maintained this load case unaltered, the picture coincides exactly for both i, ii, and iii.

The following figures (Figs. 8–10) show the deformed shapes of the frame in the full revolution path. It can be observed that for the three loading schemes the deformed shapes for the 100 revolutions are identical. It may be noted that the displacements in the beam are really large, this was induced on purpose to emphasize the fact that there is no nontrivial work generated by the fixed force, still if its magnitude is really large.

7.6. Anisotropic beam frame invariance test—follower load

Now, we consider the same elbow presented in the last example and analyze the case where the tip load is a follower

Table 5
Material properties of E-glass fiber-epoxy lamina.

E11	E22	G12	G23	$\nu12$
45.0×109	12.0×109	5.5×109	5.5×109	0.3

Table 6
Loading scheme.

Step	P_x	P_y	P_z
1	0	0	200,000
2	0	100,000	0
3	20,000	0	0
4	0	0	−200,000
5	−20,000	0	0
6	0	−100,000	0

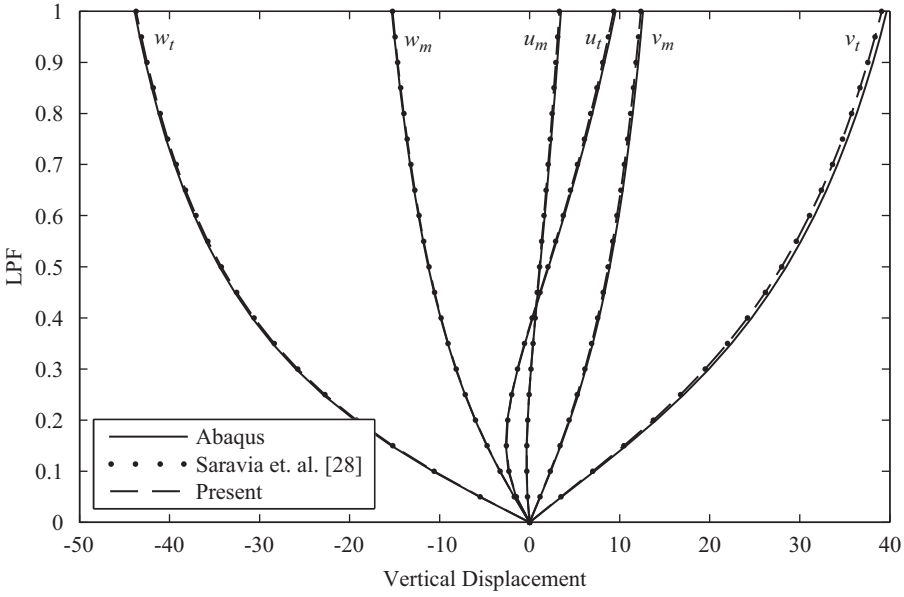

Fig. 6. Bending of an anisotropic cantilever beam—displacements vs. load proportional factor.

Table 7
Path dependency test results.

Remaining displacements							
Inc.	Elements	u	v	w	θ_1	θ_2	θ_3
5	50	-1.05×10^{-14}	-1.80×10^{-14}	0.0	0.0	0.0	-6.28×10^{-17}
	25	-9.11×10^{-15}	9.65×10^{-15}	0.0	0.0	0.0	8.29×10^{-17}
10	50	-4.49×10^{-14}	-1.25×10^{-15}	0.0	0.0	0.0	1.01×10^{-16}
	25	-1.18×10^{-14}	-4.04×10^{-15}	0.0	0.0	0.0	4.91×10^{-17}
20	50	-5.27×10^{-14}	-1.16×10^{-15}	0.0	0.0	0.0	2.23×10^{-16}
	25	-7.03×10^{-15}	5.91×10^{-19}	0.0	0.0	0.0	3.45×10^{-19}

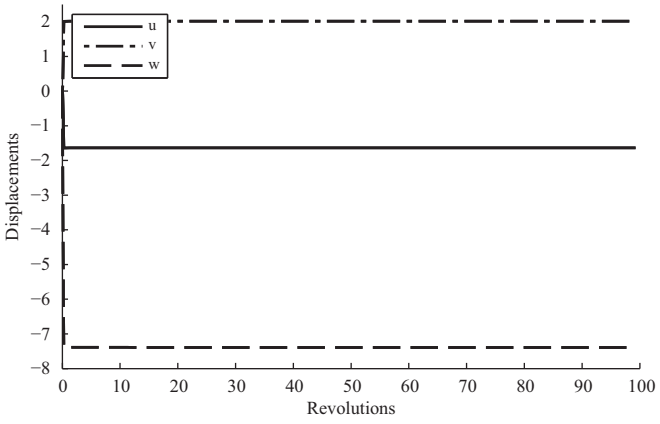

Fig. 7. Frame invariance test of an anisotropic beam—evolution of displacements with revolutions.

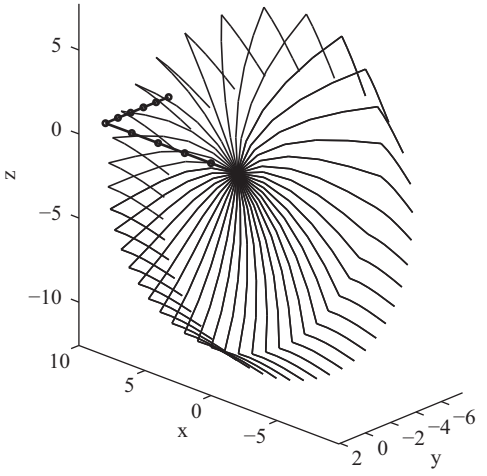

Fig. 9. Deformed anisotropic beam rotating around the y axis.

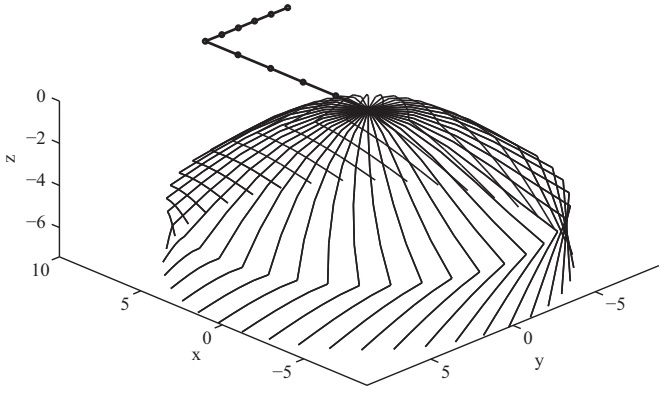

Fig. 8. Deformed anisotropic beam rotating around the z axis.

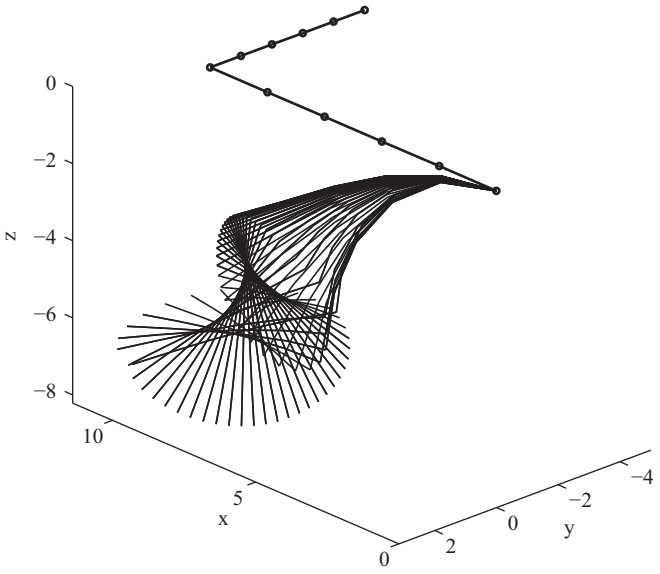

Fig. 10. Deformed anisotropic beam rotating around the x axis.

force (initially oriented in the z direction) that rotates with the frame around the y axis.

Fig. 11 shows the deformed shapes for the full rotation path of 100 revolutions, it can be observed that these deformed shapes coincide for each revolution. From this experiment, we can conclude that the present formulation is also frame-invariant. We have only presented the case where the elbow rotates about the y axis, but the remaining cases give exactly the same conclusion.

Finally we show in Fig. 12 the evolution of displacements for both the fixed force and the follower force.

As it can be seen from Fig. 12, the case with follower force exactly coincides with the case of non-follower force. It is clear that both u, v and w remain unchanged as the full revolution path evolves.

8. Conclusions

A consistent Total Lagrangian geometrically exact nonlinear beam finite element for composite closed section thin-walled beams has been presented. The proposed formulation relied on

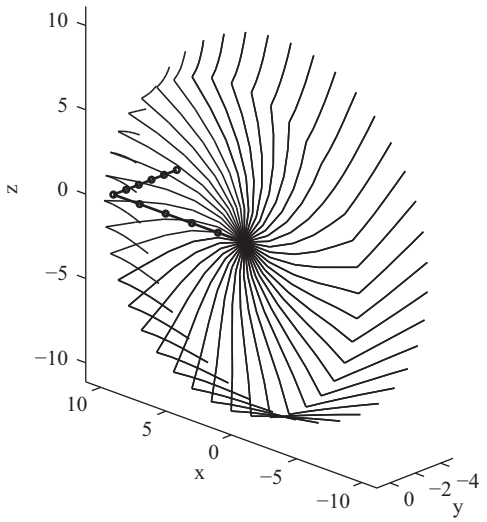

Fig. 11. Deformed anisotropic beam rotating around the *y* axis—follower force case.

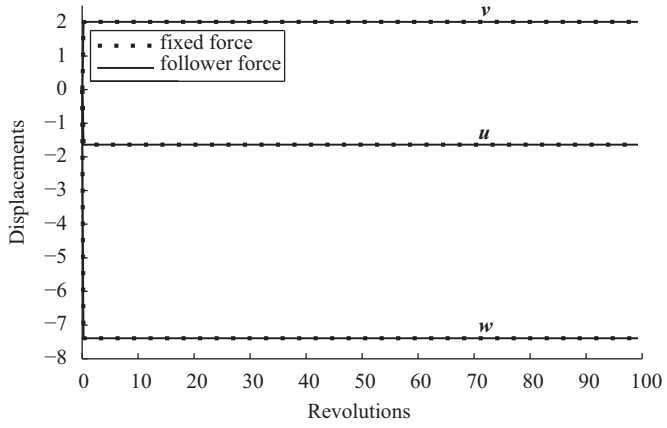

Fig. 12. Frame invariance of an anisotropic beam—follower force case.

the parametrization of the equilibrium equations in terms of the director field and its derivatives, parametrizing the finite rotations with the total rotation vector. The weak form of equilibrium was written in terms of generalized strains, which result from a dual transformation of the rectangular Green–Lagrange strains. The variables work conjugate to the generalized strains, i.e. the generalized beam forces, were deduced from the curvilinear shell stresses before the obtention of the weak form.

The main capability of the proposed formulation is the possibility of handling composite materials. Since the cross section properties can be obtained analytically, the proposed approach is attractive to be used in optimization problems of composite beams with finite deformation such as helicopter rotor blades and wind turbine blades.

Representative numerical experiments showed that the presented thin-walled beam formulation has a very good correlation against existing geometrically exact isotropic beam finite elements. For composite materials, the correlation against 3D shell models was also very good.

It has been shown that the present implementation maintains the path independence and frame invariance properties of the finite element formulation and that interpolated rotations cannot be fully avoided if it is desired to derive consistent tangential tensors.

Acknowledgments

The authors wish to acknowledge the supports from Secretaría de Ciencia y Tecnología of Universidad Tecnológica Nacional and CONICET.

Appendix A

A.1. Beam forces

The explicit expression of the beam forces vector gives

$$\boldsymbol{S}=\begin{bmatrix} N\\ M_2\\ M_3\\ Q_2\\ Q_3\\ T\\ P_2\\ P_3\\ P_{23}\end{bmatrix}=\int_S \begin{pmatrix} N_{xx}\\ M_{xx}\overline{\xi}_2'+N_{xx}\overline{\xi}_3\\ -M_{xx}\overline{\xi}_3'+N_{xx}\overline{\xi}_2\\ N_{xs}\overline{\xi}_2'-N_{xn}\overline{\xi}_3'\\ N_{xn}\overline{\xi}_2'+N_{xs}\overline{\xi}_3'\\ -M_{xs}(\overline{\xi}_2'^2+\overline{\xi}_3'^2)+N_{xs}(\overline{\xi}_3'\overline{\xi}_2-\overline{\xi}_2'\overline{\xi}_3)+N_{xn}(\overline{\xi}_2'\overline{\xi}_2+\overline{\xi}_3'\overline{\xi}_3)\\ -M_{xx}\overline{\xi}_3'\overline{\xi}_2+\frac{1}{2}N_{xx}\overline{\xi}_2^2\\ M_{xx}\overline{\xi}_2'\overline{\xi}_3+\frac{1}{2}N_{xx}\overline{\xi}_3^2\\ N_{xx}\overline{\xi}_2\overline{\xi}_3+M_{xx}(\overline{\xi}_2'\overline{\xi}_2-\overline{\xi}_3'\overline{\xi}_3)\end{pmatrix} ds, \tag{A1}$$

where N is the axial beam force, M_2 and $M_3$are the beam flexural moments, Q_2 and Q_3 are beam shear forces, T is the beam torsion moment and P_2, P_3 and P_{23} are high order flexural moments.

References

[1] Reissner E. On finite deformations of space-curved beams. Zeitschrift für Angewandte Mathematik und Physik (ZAMP) 1981;32:734–44.
[2] Bathe K-J, Bolourchi S. Large displacement analysis of three-dimensional beam structures. International Journal for Numerical Methods in Engineering 1979;14:961–86.
[3] Simo JC. A finite strain beam formulation. The three-dimensional dynamic problem. Part I. Computer Methods in Applied Mechanics and Engineering 1985;49:55–70.
[4] Simo JC, Vu-Quoc L. A three-dimensional finite-strain rod model. Part II: computational aspects. Computer Methods in Applied Mechanics and Engineering 1986;58:79–116.
[5] Simo JC, Vu-Quoc L. On the dynamics in space of rods undergoing large motions—A geometrically exact approach. Computer Methods in Applied Mechanics and Engineering 1988;66:125–61.
[6] Cardona A, Geradin M. A beam finite element non-linear theory with finite rotations. International Journal for Numerical Methods in Engineering 1988;26:2403–38.
[7] Simo JC, Vu-Quoc L. A geometrically-exact rod model incorporating shear and torsion-warping deformation. International Journal of Solids and Structures 1991;27:371–93.
[8] Ibrahimbegovic A. On finite element implementation of geometrically nonlinear Reissner's beam theory: three-dimensional curved beam elements. Computer Methods in Applied Mechanics and Engineering 1995;122:11–26.
[9] Ibrahimbegovic A. On the choice of finite rotation parameters. Computer Methods in Applied Mechanics and Engineering 1997;149:49–71.
[10] Gruttmann F, Sauer R, Wagner W. A geometrical nonlinear eccentric 3D-beam element with arbitrary cross-sections. Computer Methods in Applied Mechanics and Engineering 1998;160:383–400.
[11] Gruttmann F, Sauer R, Wagner W. Theory and numerics of three-dimensional beams with elastoplastic material behaviour. International Journal for Numerical Methods in Engineering 2000;48:1675–702.
[12] Auricchio F, Carotenuto P, Reali A. On the geometrically exact beam model: a consistent, effective and simple derivation from three-dimensional finite-elasticity. International Journal of Solids and Structures 2008;45:4766–81.
[13] Crisfield M, Jelenic G. Objectivity of strain measures in the geometrically exact three-dimensional beam theory and its finite-element implementation. Proceedings of the Royal Society of London. Series A: Mathematical, Physical and Engineering Sciences 1999;455:1125–47.
[14] Jelenic G, Crisfield MA. Geometrically exact 3D beam theory: implementation of a strain-invariant finite element for statics and dynamics. Computer Methods in Applied Mechanics and Engineering 1999;171:141–71.
[15] Ibrahimbegovic A, Taylor R. On the role of frame-invariance in structural mechanics models at finite rotations. Computer Methods in Applied Mechanics and Engineering 2002;191:5159–76.

[16] Betsch P, Steinmann P. Frame-indifferent beam finite elements based upon the geometrically exact beam theory. International Journal for Numerical Methods in Engineering 2002;54:1775–88.
[17] Armero F, Romero I. On the objective and conserving integration of geometrically exact rod models. In: Proceedings of the Trends in computational structural mechanics, CIMNE, Barcelona, Spain; 2001.
[18] Romero I, Armero F. An objective finite element approximation of the kinematics of geometrically exact rods and its use in the formulation of an energy-momentum conserving scheme in dynamics. International Journal for Numerical Methods in Engineering 2002;54:1683–716.
[19] Ghosh S, Roy D. A frame-invariant scheme for the geometrically exact beam using rotation vector parametrization. Computational Mechanics 2009;44:103–18.
[20] Sansour C, Wagner W. Multiplicative updating of the rotation tensor in the finite element analysis of rods and shells—a path independent approach. Computational Mechanics 2003;31:153–62.
[21] Mäkinen J. Total Lagrangian Reissner's geometrically exact beam element without singularities. International Journal for Numerical Methods in Engineering 2007;70:1009–48.
[22] Hodges DH, Yu W, Patil MJ. Geometrically-exact, intrinsic theory for dynamics of moving composite plates. International Journal of Solids and Structures 2009;46:2036–42.
[23] Yu W, Hodges DH, Volovoi VV, Fuchs ED. A generalized Vlasov theory for composite beams. Thin-Walled Structures 2005;43:1493–511.
[24] Cesnik CES, Hodges DH, VABS A. New concept for composite rotor blade cross-sectional modeling. Journal of the American Helicopter Society 1997; 42:27–38.
[25] Librescu L. Thin-walled composite beams. Dordrecht: Springer; 2006.
[26] Piovan MT, Cortínez VH. Mechanics of thin-walled curved beams made of composite materials, allowing for shear deformability. Thin-Walled Structures 2007;45:759–89.
[27] Machado SP, Cortínez VH. Non-linear model for stability of thin-walled composite beams with shear deformation. Thin-Walled Structures 2005;43: 1615–45.
[28] Saravia CM, Machado SP, Cortínez VH. A geometrically exact nonlinear finite element for composite closed section thin-walled beams. Computer and Structures 2011;89:2337–51.
[29] Hodges DH. Nonlinear composite beam theory. Virginia: American Institute of Aeronautics and Astronautics, Inc; 2006.
[30] Argyris J. An excursion into large rotations. Computer Methods in Applied Mechanics and Engineering 1982;32:85–155.
[31] Bonet J, Wood RD. Nonlinear continuum mechanics for finite element analysis. Cambridge: Cambridge University Press; 1997.
[32] Barbero E. Introduction to composite material design. London: Taylor and Francis; 2008.
[33] Jones RM. Mechanics of composite materials. London: Taylor & Francis; 1999.
[34] Washizu K. Variational methods in elasticity and plasticity. Oxford: Pergamon Press; 1968.
[35] Zienkiewicz OC, Taylor RL. The finite element method. Oxford: Buttherworth-Heinemann; 2000.
[36] Betsch P. On the parametrization of finite rotations in computational mechanics A classification of concepts with application to smooth shells. Computer Methods in Applied Mechanics and Engineering 1998;155:273–305.
[37] Ritto-Corrêa M, Camotim D. On the differentiation of the Rodrigues formula and its significance for the vector-like parameterization of Reissner-Simo beam theory. International Journal for Numerical Methods in Engineering 2002;55:1005–32.
[38] Crisfield MA. Non-linear finite element analysis of solids and structures: advanced topics. John Wiley & Sons, Inc.; 1997.
[39] Ibrahimbegović A, Frey F, Kožar I. Computational aspects of vector-like parametrization of three-dimensional finite rotations. International Journal for Numerical Methods in Engineering 1995;38:3653–73.
[40] Ibrahimbegovic A, Al Mikdad M. Finite rotations in dynamics of beams and implicit time-stepping schemes. International Journal for Numerical Methods in Engineering 1998;41:781–814.
[41] Taylor R. FEAP users manual. In: Proceedings of the FEAP Berkeley; 2009.